Quandle Theoretic Knot Invariants

By

NICHOLAS CAZET
DISSERTATION

Submitted in partial satisfaction of the requirements for the degree of

DOCTOR OF PHILOSOPHY

in

Pure Mathematics

in the

OFFICE OF GRADUATE STUDIES

of the

UNIVERSITY OF CALIFORNIA

DAVIS

Approved:

Jennifer Schultens, Chair

Abigail Thompson

Eugene Gorsky

Committee in Charge

2024

Contents

Abstract

This dissertation is based on the following three publications of the author [15,16,17], focusing on quandles and their applications in knot theory.

Chapter 2 defines a family of quandles and studies their algebraic invariants. The axioms of a quandle imply that the columns of its Cayley table are permutations. The chapter studies quandles with exactly one non-trivially permuted column. Their automorphism groups, quandle polynomials, (symmetric) cohomology groups, and *Hom* quandles are studied. The quiver and cocycle invariant of links using these quandles are shown to relate to linking number.

Chapter 3 describes the triple point number of non-orientable surface-links using symmetric quandles. Analogous to a classical knot diagram, a surface-link can be generically projected to 3-space and given crossing information to create a broken sheet diagram. The triple point number of a surface-link is the minimal number of triple points among all broken sheet diagrams that lift to that surface-link. The chapter generalizes a family of Oshiro to show that there are non-split surface-links of arbitrarily many trivial components whose triple point number can be made arbitrarily large.

Chapter 4 focuses on the triple point number of surface-links found in Yoshikawa's table. Yoshikawa made an enumeration of knotted surfaces in R^4 with ch-index 10 or less. This remarkable table is the first to tabulate knotted surfaces analogous to the classical prime knot table. This chapter compiles the known triple point numbers of the surface-links represented in Yoshikawa's table and calculates or provides bounds on the triple point number of the remaining surface-links.

Chapter 5 is included to study quandle invariants of knotoids. The chapter focuses on the chirality of knotoids using shadow quandle colorings and the shadow quandle cocycle invariant. The shadow coloring number and the shadow quandle cocycle invariant is shown to distinguish infinitely many knotoids from their mirrors. Specifically, the knot-type knotoid 3_1 is shown to be chiral. The weight of a quandle 3-cocycle is used to calculate the crossing numbers of infinitely many multi-linkoids.

Acknowledgments

I thank my parents Craig and Julie Cazet for their continued generous support.

CHAPTER 1

Introduction

Quandles were independently introduced by Joyce and Matveev in the 1980's [35, 46]. They showed that the fundamental knot quandle is an algebraic invariant that distinguishes knots up to mirror reflection. The texts [10, 22, 38, 50] give a good account of definitions and applications of quandles in (surface-) knot theory.

In their seminal article defining quandle cohomology [7], Carter et al. defined the quandle cocycle invariant and used it to show that the 2-twist-spun trefoil is not isotopic to its orientation reverse. Notable use of the invariant also includes [14,31,39,58,59,60]. Using a quandle 2-cocycle, this invariant can be defined for classical links.

A *surface-link* is a smoothly embedded closed surface in $\mathbb{R}^4$. A *2-knot* is a surface-knot diffeomorphic to the 2-sphere, and a *surface-knot* will mean a connected surface-knot. Two surface-links are *equivalent* if they are related by an ambient isotopy in the smooth category. For an orthogonal projection $p : \mathbb{R}^4 \to \mathbb{R}^3$, a surface-knot F can be perturbed slightly so that $p(F)$ is a generic surface. Each point of $p(F)$ has a neighborhood in 3-space diffeomorphic to $\mathbb{R}^3$ such that the image of the generic surface under the diffeomorphism looks like 1, 2, or 3 coordinate planes or the cone on a figure 8 (Whitney umbrella). These points are called regular points, double points, triple points, and branch points. Triple points and branch points are isolated while double points are not and lie on curves called *double point curves*. The union of non-regular points is the *singular set* of the generic surface [10], [38].

A *broken sheet diagram* of a surface-link F is a generic projection $p(F)$ with consistently broken sheets along double point curves, see Figure 1.1 and [12]. The sheet that lifts below the other, with respect to a height function determined by the direction of the orthogonal projection p, is locally broken at the singular set. All surface-links admit a broken sheet diagram, and all broken sheet diagrams lift to surface-knots in 4-space. Although, not all compact, generic surfaces in 3-space can be given a broken sheet structure [13].

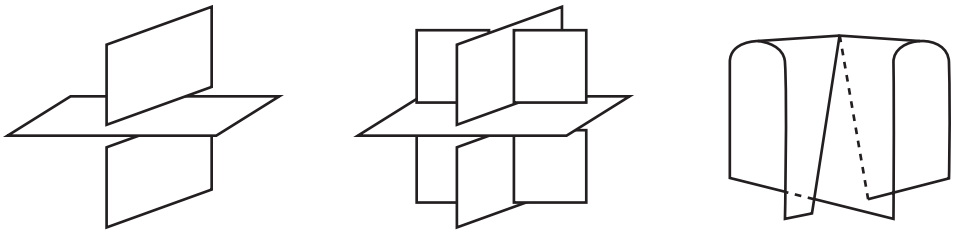

FIGURE 1.1. Local images of a double point, triple point, and branch point.

The minimal number of triple points among all generic projections of a surface-link F is called the *triple point number* of F and is denoted $t(F)$. The triple point number has an analogy to the crossing number of a classical knot. Although it is unknown if the crossing number of classical knots is additive under connected sum, Satoh showed that the connected sum of the n-twist-spin of a 2-bridge knot with the non-orientable trivial surface-knot of genus 3 and normal Euler number ± 2 produces a surface-knot whose triple point number is zero while it is known that these twist-spins have positive triple point number [57].

Since their introduction in 2012 by Turaev [62], knotoids and their invariants have generated much interest, for example see [25, 27, 43, 45]. Knotoids are considered generalized knots and best understood as knotted arcs. Gügümcü, Kauffman, and Lambropoulou give an excellent account of knotoid research from its inception until 2019 in [28]. Included in their exposition is the interest in knotoids among mathematical biologists for modeling open protein chains, for example see [2, 20, 24, 26]. The equivalence put on knotoid diagrams is defined using Reidemeister moves away from the endpoints, and quandles are used to define knot invariants because diagram colorings behave well under Reidmeister moves. Therefore, quandle invariants naturally extend to knotoids.

The first formal study of quandles in the context of knotoids was done by Gügümcü and Nelson in [29]. They showed that the biquandle counting invariant can detect mirror images of knotoids. Later, Gügümcü, Nelson, and Oyamguchi introduced the biquandle bracket of knotoids and showed that this invariant is stronger than the counting invariant [30].

CHAPTER 2

Quandles With One Non-Trivial Column

DEFINITION 2.0.1. *A quandle is a set X with a binary operation $(x, y) \mapsto x * y$ such that*

(i) for any $x \in X$, $x * x = x$,

(ii) for any $x, y \in X$, there exists a unique $z \in X$ such that $z * y = x$, and

(iii) for any $x, y, z \in X$, $(x * y) * z = (x * z) * (y * z)$.

There are 3 quandles of order 3, the trivial T_3, the dihedral R_3, and P_3. The quandle P_3 fits into a family of quandles P_n^σ defined in this paper having only one non-trivially permuted column in their Cayley tables. Several second and third homology groups of P_n^σ are calculated since quandle cocycles define link invariants. In addition, Hom quandles between specific P_n^σ, the automorphism groups of P_n^σ, and the quandle polynomials of P_n^σ are calculated.

Section 2.1 defines P_n^σ and studies their algebraic invariants. Section 2.2 computes several cohomology groups of P_n^σ. Section 2.3 analyzes the quandle quiver and cocycle invariant of links using P_n^σ.

For any $x, y \in X$, let $x \overline{*} y$ be the unique $z \in X$ such that $z * y = x$.

DEFINITION 2.0.2 ([37]). *An involution ρ on a quandle X is good if $\rho(x * y) = \rho(x) * y$ and $x * \rho(y) = x \overline{*} y$ for all $x, y \in X$. Such a pair (X, ρ) is a symmetric quandle.*

EXAMPLE 2.0.3 ([37]). *Conjugation on a group $g * h = h^{-1}gh$ defines a quandle. The inverse map $\rho(g) = g^{-1}$ is a good involution.*

EXAMPLE 2.0.4. *The trivial quandle $T_n = \{0, 1, \ldots, n-1\}$ of order n is defined by $x * y = x$ for all $x, y \in T_n$. Any involution on T_n is good.*

EXAMPLE 2.0.5. *The operation $x * y \equiv 2y - x \mod n$ on $\mathbb{Z}_n$ gives the dihedral quandle R_n. Kamada and Oshiro classified all good involutions on R_n in [40].*

Finite quandles have Cayley tables. The table's entries (α_{ij}) are given by $\alpha_{ij} = i * j$. The axioms of a quandle imply that $\alpha_{ii} = i$ and that the columns of the table represent permutations. Table 2.1 gives the Cayley tables of all order 3 quandles.

	0	1	2
0	0	0	0
1	1	1	1
2	2	2	2

	0	1	2
0	0	2	1
1	2	1	0
2	1	0	2

	0	1	2
0	0	0	0
1	2	1	1
2	1	2	2

TABLE 2.1. Cayley tables of T_3, R_3, and P_3.

2.0.1. Automorphism Groups. A *quandle homomorphism* satisfies $f(x * y) = f(x) * f(y)$. Under the operation of composition, the bijective endomorphisms on a quandle X constitute its automorphism group $Aut(X)$. For every $y \in X$, let $S_y(x) = x * y$. The second axiom of a quandle implies that S_y is a bijection for any $y \in X$. The group generated by the permutations S_y is the quandle's inner automorphism group $Inn(X)$. Recent articles studying these groups include [3, 4, 21, 32].

2.0.2. Quandle Polynomials. Nelson introduced a two-variable polynomial invariant of finite quandles in [48].

DEFINITION 2.0.6. *Let X be a finite quandle. For any element $x \in X$, let*

$$c(x) = |\{y \in X \ : \ y * x = y\}|, \text{ and } r(x) = |\{y \in X : x * y = x\}|.$$

The quandle polynomial of X is $qp_X(s,t) = \sum_{x \in X} s^{r(x)} t^{c(x)}$.

He later generalized the polynomial in [49].

2.0.3. *Hom* Quandles.

DEFINITION 2.0.7. *A quandle A is abelian or medial if for all $x, y, z, w \in Q$,*

$$(x * y) * (z * w) = (x * z) * (y * w).$$

Crans and Nelson showed that when A is an abelian quandle the set of quandle homomorphisms $Hom(X, A)$ from a quandle X to A has a natural quandle structure [19].

THEOREM 2.0.8 (Crans, Nelson '14 [19]). *Let X and A be quandles. If A is abelian, then $Hom(X, A)$ is an abelian quandle under the pointwise operation $(f * g)(x) = f(x) * g(x)$. Let X be a finitely generated quandle and A an abelian quandle. Then $Hom(X, A)$ is isomorphic to a subquandle of A^c where c is the minimal number of generators of X. Identify an element $f \in Hom(X, A)$ with the c-tuple*

$$(f(x_1), \ldots, f(x_c)).$$

The pointwise operation on $Hom(X, A)$ agrees with the componentwise operation on the product A^c.

For a finite quandle $X = \{0, 1, \ldots, n-1\}$, it is sufficient to classify the componentwise quandle structure of the n-tuples $(f(0), f(1), \ldots, f(n-1))$ to determine the quandle structure of $Hom(X, A)$. *Hom* and abelian quandles were recently studied in [6, 33, 34, 44].

2.0.4. Quandle Coloring Number. Let X be a finite quandle. Assigning X elements to the arcs of an oriented link diagram so that each crossing satisfies the quandle coloring condition of Figure 2.1 is called a *quandle coloring*, specifically an *X-coloring*. The axioms of a quandle imply that an X-coloring uniquely extends to another after any of the 3 Reidemeister moves, see [10, 22, 38]. For a finite quandle X, the *quandle coloring number* $col_X(L)$ is a link invariant and equal to the number of X-colorings of any diagram of L.

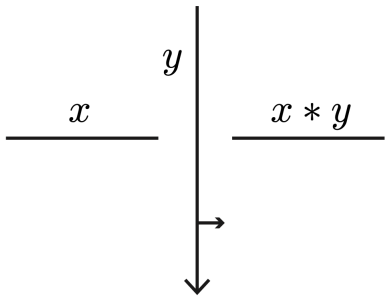

FIGURE 2.1. Quandle coloring condition.

2.0.5. Quandle Quivers. A quandle endomorphism $f \in End(X)$ acts on an X-coloring of a link diagram by replacing the arcs' colors by their images under f. Cho and Nelson introduced the *quandle quiver invariant* of links enhancing and categorifying the coloring number [18].

DEFINITION 2.0.9. *Let X be a finite quandle and $S \subset End(X)$. The quandle quiver $\mathcal{Q}_X^S(L)$ of a link L is a directed graph with vertices representing the X-colorings of L and directed edges representing the action of S on its colorings.*

Two quivers are isomorphic if there exists a bijection f between their vertices that extends to a bijection F between their edges, $F(v_1v_2) = f(v_1)f(v_2)$ for every edge v_1v_2.

THEOREM 2.0.10. *The quandle quiver $\mathcal{Q}_{T_n}^S(L)$ is determined by the number of components in L.*

PROOF. Let L be a link with k components. A T_n-coloring of L is k independent choices of colors, one for each component. Let $\varphi : \pi_0(L) \to \pi_0(L')$ be a bijection between the components of L and the components of another link L' with k components. The bijection φ extends to a bijection $\Phi : \mathrm{Col}_{T_n}(L) \to \mathrm{Col}_{T_n}(L')$. Let $f \in \mathrm{End}(T_n)$. Sending the edge connecting the colorings c and $f \circ c$ to the edge connecting $\Phi(c)$ and $\Phi(f \circ c)$ defines a quiver isomorphism. □

THEOREM 2.0.11 (Taniguchi '20 [61]). *Let L and L' be oriented link diagrams and p be a prime. For any $S \subseteq End(R_p)$, the quandle quivers $Q_{R_p}^S(L)$ and $Q_{R_p}^S(L')$ are isomorphic if and only if $col_{R_p}(L) = col_{R_p}(L')$.*

Recent studies of quandle quivers include [5, 42, 64].

2.0.6. Quandle Cohomology. Quandle cohomology was introduced by Carter, Jelsovsky, Kamada, Langford, and Saito to study classical oriented links and oriented surface-links [7]. Symmetric quandle cohomology was later introduced by Kamada to study classical unoriented links and unoriented surface-links [37].

Let X be a quandle. Let $C_n(X)$ be the free abelian group generated by X^n when $n \geq 1$ and $C_n(X) = 0$ when $n < 1$. Define the boundary homomorphism $\partial_n : C_n(X) \to C_{n-1}(X)$ by

$$\partial_n(x_1, \ldots, x_n) = \sum_{i=1}^{n} (-1)^i \{(x_1, \ldots, \hat{x}_i, \ldots, x_n) - (x_1 * x_i, \ldots, x_{i-1} * x_i, \hat{x}_i, x_{i+1}, \ldots, x_n)\}$$

for $n > 1$ and $\partial_n = 0$ for $n \leq 1$. Then $C_*(X) = \{C_n(X), \partial_n\}$ is a chain complex [7, 8, 10, 38]. For $n \geq 2$, let $D_n^Q(X)$ be the subgroup of $C_n(X)$ generated by the elements

$$\bigcup_{i=1}^{n-1} \{(x_1, \ldots, x_n) \in X^n \mid x_i = x_{i+1}\},$$

and for $n < 2$, let $D_n^Q(X) = 0$. For a good involution $\rho : X \to X$, let $D_n^\rho(X)$ be the subgroup of $C_n(X)$ generated by the elements

$$\bigcup_{i=1}^{n} \{(x_1, \ldots, x_n) + (x_1 * x_i, \ldots, x_{i-1} * x_i, \rho(x_i), x_{i+1}, \ldots, x_n) \mid x_1, \ldots, x_n \in X^n\},$$

for $n \geq 1$ and $D_n^\rho(X) = 0$ for $n < 1$. Then $D_*^Q(X) = \{D_n^Q(X), \partial_n\}$ and $D_*^\rho(X) = \{D_n^\rho(X), \partial_n\}$ are subcomplexes of $C_*(X)$ [40]. Let $C_*^Q(X) = C_*(X)/D_*^Q(X)$ and $C_*^{Q,\rho}(X) = C_*(X)/(D_*^Q(X) + D_*^\rho(X))$

For an abelian group A, the cohomology groups of the complexes

$$C_*^Q(X; A) = C_*^Q(X) \otimes A \text{ and } C_*^{Q,\rho}(X; A) = C_*^{Q,\rho} \otimes A$$

are the *quandle cohomology groups* $H_Q^*(X; A)$ and the *symmetric quandle cohomology groups* $H_{Q,\rho}^*(X; A)$ of X.

LEMMA 2.0.11.1 ([7,8,10,38]). *Let X be a quandle and A an abelian group. A homomorphism $f : C_2(X) \to A$ is a quandle 2-cocycle of X if the following conditions are satisfied:*

(i) For any $x_0, x_1, x_2 \in X$,

$$f(x_0, x_1) + f(x_0 * x_1, x_2)$$
$$- f(x_0, x_2) - f(x_0 * x_2, x_1 * x_2) = 0$$

(ii) For all $x \in X$, $f(x, x) = 0$.

2.0.7. Quandle Cocycle Invariant. For a finite quandle X, let θ be a quandle 2-cocycle with coefficients in an abelian group A written multiplicatively. Let L be an X-colored link diagram and C denote the set of its crossings. For $c \in C$, suppose that x is the color assigned to the under arc for which the orientation normal of the over arc points away from and y is the color of the over arc as in Figure 2.1. Define $\theta_c = \theta(x, y)^\epsilon$ to be the θ-weight of the X-colored crossing c where ϵ is $+1$ if the crossing is positive and -1 if the crossing is negative. The θ-weight of an X-colored link diagram is the product of all θ_c's. The quandle cocycle invariant is the formal sum of all θ-weights.

The *quandle cocycle invariant* of L is

$$\Phi_\theta(L) = \sum_{X\text{-colorings}} \prod_{c \in C} \theta_c \in \mathbb{Z}[A].$$

A proof that $\Phi_\theta(L)$ does not depend on the diagram of L can be found in [7, 10, 38].

2.1. The Quandle P_n^σ

Let S_n be the symmetric group on the first n positive integers and $\sigma \in S_n$ a permutation. Define the operation $*$ on $P_n^\sigma = \{0, 1, 2, \ldots, n\}$ by

$$x * y = \begin{cases} x & y \neq 0 \\ \sigma(x) & y = 0, x \neq 0 \\ 0 & y = 0, x = 0. \end{cases}$$

This is also defined by permuting the positive entries in the first column of the trivial quandle T_{n+1}'s Cayley table with respect to σ, see Table 2.2.

	0	1	2	$\cdots$	n
0	0	0	0	$\cdots$	0
1	$\sigma(1)$	1	1	$\cdots$	1
2	$\sigma(2)$	2	2	$\cdots$	2
$\vdots$	$\vdots$	$\vdots$	$\vdots$	$\ddots$	$\vdots$
n	$\sigma(n)$	n	n	$\cdots$	n

TABLE 2.2. Cayley table of P_n^σ.

PROPOSITION 2.1.1. *$(P_n^\sigma, *)$ is a quandle.*

PROOF. The diagonal of its Cayley table shows that the first axiom is satisfied and since each column is a permutation the second axiom satisfied. The third axiom

$$(x * y) * z = (x * z) * (x * z)$$

follows from a case study, see Table 2.3. □

If $\sigma = id$, then P_n^σ is the trivial quandle T_{n+1}.

x	y	z	$(x*y)*z=(x*z)*(y*z)$
$+$	$+$	$+$	$x=x$
$+$	$+$	0	$\sigma(x)=\sigma(x)$
$+$	0	$+$	$\sigma(x)=\sigma(x)$
0	$+$	$+$	$0=0$
$+$	0	0	$\sigma^2(x)=\sigma^2(x)$
0	$+$	0	$0=0$
0	0	$+$	$0=0$
0	0	0	$0=0$

TABLE 2.3. The cases of Proposition 2.1.1.

LEMMA 2.1.0.1. *If $\sigma \neq id$, then any quandle isomorphism between P_n^σ and P_n^τ fixes 0.*

PROOF. Suppose that f is an isomorphism with $f(0) \neq 0$. For any $a \neq 0$, $f(\sigma(a)) = f(a*0) = f(a)*f(0) = f(a)$ implying that $\sigma(a) = a$.

□

THEOREM 2.1.1. *$P_n^\sigma \cong P_n^\tau$ if and only if σ is conjugate to τ.*

PROOF. Suppose that $f : P_n^\sigma \to P_n^\tau$ is a quandle isomorphism and $x \in P_n$ is positive. Lemma 2.1.0.1 implies that $f(0) = 0$. Therefore, $f(\sigma(x)) = f(x*0) = f(x)*f(0) = f(x)*0 = \tau(f(x))$, i.e. $\sigma = f^{-1}\tau f$ on the positive integers.

Now suppose that $\sigma = h^{-1}\tau h$ for some permutation $h \in S_n$. Extend h to $h' : P_n^\sigma \to P_n^\tau$ by setting $h'(0) = 0$ and $h'(x) = h(x)$ for $x \neq 0$. A case study shows that h' is a quandle homomorphism thus isomorphism. If $a, b \neq 0$, then $h'(a*b) = h'(a) = h(a) = h(a)*h(b) = h'(a)*h'(b)$ since $h(b) \neq 0$. If $a \neq b = 0$, then $h'(a*b) = h(\sigma(a)) = \tau(h(a)) = h(a)*0 = h'(a)*h'(b)$. If $a = 0$, then $h'(a*b) = h'(0) = 0 = 0*h'(b) = h'(a)*h'(b)$ for any b.

□

THEOREM 2.1.2. *If $\sigma \neq id$, then $Aut(P_n^\sigma) \cong C_{S_n}(\sigma)$ and $Inn(P_n^\sigma) \cong \mathbb{Z}_{|\sigma|}$ where $C_{S_n}(\sigma)$ denotes σ's centralizer and $|\sigma|$ is the order of σ.*

PROOF. For any $f \in Aut(P_n^\sigma)$, let f_+ be its restriction to $P_n^\sigma \setminus \{0\} = S_n$. Lemma 2.1.0.1 implies that any two automorphisms f and g satisfy $(g \circ f)_+ = g_+ \circ f_+$. For any positive $x \in P_n^\sigma$,

$$f_+(\sigma(x)) = f_+(x*0) = f(x*0) = f(x)*f(0) = f_+(x)*0 = \sigma(f_+(x)),$$

so $f_+ \in C_{S_n}(\sigma)$. Therefore, the restriction map $f \mapsto f_+$ is a group homomorphism from $Aut(P_n^\sigma)$ to $C_{S_n}(\sigma)$.

For any $g \in C_{S_n}(\sigma)$, let $g_0 : P_n^\sigma \to P_n^\sigma$ be its extension where $g_0(x) = g(x)$ for $x \neq 0$ and $g_0(0) = 0$. A case study shows that the bijection g_0 is an automorphism. If $a, b \neq 0$, then $g_0(a * b) = g(a) = g(a) * g(b) = g_0(a) * g_0(b)$. If $a \neq b = 0$, then

$$g_0(a * b) = g_0(\sigma(a)) = g(\sigma(a)) = \sigma(g(a)) = \sigma(g_0(a)) = g_0(a) * 0 = g_0(a) * g_0(0).$$

If $b \neq a = 0$ or $a = b = 0$, then $g_0(a * b) = 0 = g_0(a) * g_0(b)$. Altogether, g_0 is an automorphism and the extension map $g \mapsto g_0$ is inverse to the restriction map $f \mapsto f_+$.

There are two permutations that generate $Inn(P_n^\sigma)$, $S_0(x) = x * 0 = \sigma(x)$ and $S_{a\neq 0}(x) = x * a = x$. These generate the cyclic group of the same order as σ.

□

THEOREM 2.1.3. *Let α be the number of positive integers fixed by a non-trivial σ. The quandle polynomial of P_n^σ is*

$$qp_{P_n^\sigma}(s,t) = \alpha s^{n+1}t^{n+1} + (n-\alpha)s^n t^{n+1} + s^{n+1}t^{1+\alpha}.$$

PROOF. For a positive x fixed by σ, $r(x) = c(x) = n + 1$. If x is positive and not fixed by σ, then $r(x) = n$ and $c(x) = n + 1$. Finally, $r(0) = n + 1$ and $c(0) = 1 + \alpha$. □

REMARK 2.1.1. *The quandle polynomial distinguishes the isomorphism classes of P_n^σ and P_n^τ if and only if σ and τ have a different number of fixed points.*

LEMMA 2.1.3.1. *P_n^σ is abelian for any σ.*

PROOF. The abelian condition

$$(x * y) * (z * w) = (x * z) * (y * w)$$

is verified by checking all permutations of the variables being positive or zero. If $x = 0$, the equation simplifies to $0 = 0$ for any y, z, and w. Table 2.4 verifies the cases where $x \neq 0$.

□

x	y	z	w	$(x*y)*(z*w)=(x*z)*(y*w)$
$+$	$+$	$+$	$+$	$x=x$
$+$	0	0	0	$\sigma^2(x)=\sigma^2(x)$
$+$	$+$	0	0	$\sigma(x)=\sigma(x)$
$+$	0	$+$	0	$\sigma(x)=\sigma(x)$
$+$	0	0	$+$	$\sigma^2(x)=\sigma^2(x)$
$+$	$+$	$+$	0	$x=x$
$+$	$+$	0	$+$	$\sigma(x)=\sigma(x)$
$+$	0	$+$	$+$	$\sigma(x)=\sigma(x)$

TABLE 2.4. The cases of Lemma 2.1.3.1 where $x \neq 0$.

THEOREM 2.1.4. *Let σ and σ' be n-cycles. Table 2.5 gives the Cayley table of*

$$Hom(P_n^{\sigma}, P_n^{\sigma'}).$$

PROOF. Assume that $\sigma = \sigma' = (123\cdots n)$ by Theorem 2.1.1. Let $f \in Hom(P_n^{\sigma}, P_n^{\sigma'})$. If $f(k) = 0$ for some $k \neq 0$, then

$$f(\sigma(k)) = f(k*0) = f(k)*f(0) = 0.$$

This implies that f is zero on all positive integers since σ is an n-cycle. If further $f(0) \neq 0$, then $f(0) = f(0*k) = f(0)*f(k) = f(0)*0 = \sigma'(f(0))$. Since σ' has no fixed pointed, $f(0) = 0$. Therefore, $f(k) = 0$ for some $k \neq 0$ only if f is the zero map.

Now suppose that $f(k)$ is positive whenever k is positive. If $f(0) = 0$, then f is determined by where it sends 1. For any positive k, $f(k) = f(\sigma^k(1)) = f(1 *^k 0) = f(1) *^k 0 = (\sigma')^k(f(1))$. If $f(0) \neq 0$, then $f(1) = f(2) = \cdots = f(n)$ since $f(\sigma(k)) = f(k*0) = f(k)*f(0) = f(k)$.

The map f is determined by its values on 0 and 1. If f is not the zero map, then $f(0) \in P_n^{\sigma'}$ and $f(1) \in P_n^{\sigma'} \setminus \{0\}$. The set $Hom(P_n^{\sigma}, P_n^{\sigma'})$ is parameterized by the tuples $(f(0), f(1))$ and its quandles structure is described in Tables 2.5 and 2.6.

□

COROLLARY 2.1.1. *Table 2.7 gives the Cayley table of $Hom(P_3, P_3)$.*

PROOF. There are 7 endomorphisms described as the triples $(f(0), f(1), f(2))$: $0 = (0,0,0), 1 = (0,1,2), 2 = (0,2,1), 3 = (1,1,1), 4 = (2,2,2), 5 = (1,2,2), 6 = (2,1,1)$.

□

	(0,0)	(0,1)	(0,2)	$\cdots$	$(0,n)$	(1,1)	$\cdots$
(0,0)	(0,0)	(0,0)	(0,0)	$\cdots$	(0,0)	(0,0)	$\cdots$
(0,1)	(0,2)	(0,1)	(0,1)	$\cdots$	(0,1)	(0,1)	$\cdots$
(0,2)	(0,3)	(0,2)	(0,2)	$\cdots$	(0,2)	(0,2)	$\cdots$
$\vdots$	$\vdots$	$\vdots$	$\vdots$	$\ddots$	$\vdots$	$\vdots$	$\ddots$
$(0,n)$	(0,1)	$(0,n)$	$(0,n)$	$\cdots$	$(0,n)$	$(0,n)$	$\cdots$
(1,1)	(2,2)	(2,1)	(2,1)	$\cdots$	(2,1)	(1,1)	$\cdots$
(1,2)	(2,3)	(2,2)	(2,2)	$\cdots$	(2,2)	(1,2)	$\cdots$
$\vdots$	$\vdots$	$\vdots$	$\vdots$	$\ddots$	$\vdots$	$\vdots$	$\ddots$
$(1,n)$	(2,1)	$(2,n)$	$(2,n)$	$\cdots$	$(2,n)$	$(1,n)$	$\cdots$
$(2,1)$	(3,2)	(3,1)	(3,1)	$\cdots$	(3,1)	$(2,1)$	$\cdots$
$(2,2)$	(3,3)	(3,2)	(3,2)	$\cdots$	(3,2)	$(2,2)$	$\cdots$
$\vdots$	$\vdots$	$\vdots$	$\vdots$	$\ddots$	$\vdots$	$\vdots$	$\ddots$
$(2,n)$	(3,1)	$(3,n)$	$(3,n)$	$\cdots$	$(3,n)$	$(2,n)$	$\cdots$
$\vdots$	$\vdots$	$\vdots$	$\vdots$	$\ddots$	$\vdots$	$\vdots$	$\ddots$
$(n,1)$	(1,2)	(1,1)	(1,1)	$\cdots$	(1,1)	$(n,1)$	$\cdots$
$(n,2)$	(1,3)	(1,2)	(1,2)	$\cdots$	(1,2)	$(n,2)$	$\cdots$
$\vdots$	$\vdots$	$\vdots$	$\vdots$	$\ddots$	$\vdots$	$\vdots$	$\ddots$
(n,n)	(1,1)	$(1,n)$	$(1,n)$	$\cdots$	$(1,n)$	(n,n)	$\cdots$

TABLE 2.5. Cayley table of $Hom(P_n^{n-cycle}, P_n^{n-cycle})$, 1 of 2.

2.2. Cohomology Groups of P_n^σ

The goal of this section is to compute $H^2_Q(P_n^\sigma; A)$, and classify the good involutions of P_n^σ to compute $H^2_{Q,\rho}(P_3; \mathbb{Z}_2)$. The computations will follow the notation of [7] where the coefficient group A is taken to be $\mathbb{Z}$, $\mathbb{Z}_p$, or $\mathbb{Q}$.

THEOREM 2.2.1. *Let k be the number of cycles in σ. For any A,*

$$H^2_Q(P_n^\sigma; A) = A^{k^2+k}.$$

PROOF. A 2-cocycle $\phi \in Z^2(P_n^\sigma; A)$ can be expressed as $\phi = \sum_{i,j \in P_n^\sigma} C_{(i,j)}\chi_{(i,j)}$ such that

$$C_{(p,r)} + C_{(p*r,q*r)} = C_{(p,q)} + C_{(p*q,r)},$$

and $C_{(p,p)} = 0$ for all $p, q, r \in P_n^\sigma$, see Lemma 2.0.11.1. Checking all permutations of p, q, and r being 0 determines relations among the coefficients, see Table 2.8.

	$(1,n)$	$(2,1)$	$\cdots$	$(2,n)$	$\cdots$	$(n,1)$	$\cdots$	(n,n)
(0,0)	(0,0)	(0,0)	$\cdots$	(0,0)	$\cdots$	(0,0)	$\cdots$	(0,0)
(0,1)	(0,1)	(0,1)	$\cdots$	(0,1)	$\cdots$	(0,1)	$\cdots$	(0,1)
(0,2)	(0,2)	(0,2)	$\cdots$	(0,2)	$\cdots$	(0,2)	$\cdots$	(0,2)
$\vdots$	$\vdots$	$\vdots$	$\ddots$	$\vdots$	$\ddots$	$\vdots$	$\ddots$	$\vdots$
$(0,n)$	$(0,n)$	$(0,n)$	$\cdots$	$(0,n)$	$\cdots$	$(0,n)$	$\cdots$	$(0,n)$
(1,1)	(1,1)	(1,1)	$\cdots$	(1,1)	$\cdots$	(1,1)	$\cdots$	(1,1)
(1,2)	(1,2)	(1,2)	$\cdots$	(1,2)	$\cdots$	(1,2)	$\cdots$	(1,2)
$\vdots\vdots$	$\vdots$	$\ddots$	$\vdots$	$\ddots$	$\vdots$	$\ddots$	$\vdots$	
$(1,n)$	$(1,n)$	$(1,n)$	$\cdots$	$(1,n)$	$\cdots$	$(1,n)$	$\cdots$	$(1,n)$
$(2,1)$	$(2,1)$	$(2,1)$	$\cdots$	$(2,1)$	$\cdots$	$(2,1)$	$\cdots$	$(2,1)$
$(2,2)$	$(2,2)$	$(2,2)$	$\cdots$	$(2,2)$	$\cdots$	$(2,2)$	$\cdots$	$(2,2)$
$\vdots$	$\vdots$	$\vdots$	$\ddots$	$\vdots$	$\ddots$	$\vdots$	$\ddots$	$\vdots$
$(2,n)$	$(2,n)$	$(2,n)$	$\cdots$	$(2,n)$	$\cdots$	$(2,n)$	$\cdots$	$(2,n)$
$\vdots$	$\vdots$	$\vdots$	$\ddots$	$\vdots$	$\ddots$	$\vdots$	$\ddots$	$\vdots$
$(n,1)$	$(n,1)$	$(n,1)$	$\cdots$	$(n,1)$	$\cdots$	$(n,1)$	$\cdots$	$(n,1)$
$(n,2)$	$(n,2)$	$(n,2)$	$\cdots$	$(n,2)$	$\cdots$	$(n,2)$	$\cdots$	$(n,2)$
$\vdots$	$\vdots$	$\vdots$	$\ddots$	$\vdots$	$\ddots$	$\vdots$	$\ddots$	$\vdots$
(n,n)	(n,n)	(n,n)	$\cdots$	(n,n)	$\cdots$	(n,n)	$\cdots$	(n,n)

TABLE 2.6. Cayley table of $Hom(P_n^{n-cycle}, P_n^{n-cycle})$, 2 of 2.

	0	1	2	3	4	5	6
0	0	0	0	0	0	0	0
1	2	1	1	1	1	1	1
2	1	2	2	2	2	2	2
3	4	6	6	3	3	3	3
4	3	5	5	4	4	4	4
5	6	4	4	5	5	5	5
6	5	3	3	6	6	6	6

TABLE 2.7. Cayley table of $Hom(P_3, P_3)$.

This gives the non-trivial relations

$$C_{(0,\sigma(q))} = C_{(0,q)},$$

$$C_{(\sigma(p),\sigma(q))} = C_{(p,q),}$$

$$C_{(\sigma(p),r)} = C_{(p,r)},$$

p	q	r	$C_{(p,r)} + C_{(p*r,q*r)} = C_{(p,q)} + C_{(p*q,r)}$
0	0	0	$0 = 0$
+	0	0	$C_{(p,0)} + C_{(\sigma(p),0)} = C_{(\sigma(p),0)} + C_{(p,0)}$
0	+	0	$C_{(0,q)} = C_{(0,\sigma(q))}$
0	0	+	$C_{(0,r)} = C_{(0,r)}$
+	+	0	$C_{(\sigma(p),\sigma(q))} = C_{(p,q)}$
+	0	+	$C_{(\sigma(p),r)} = C_{(p,r)}$
0	+	+	$C_{(0,r)} + C_{(0,q)} = C_{(0,q)} + C_{(0,r)}$
+	+	+	$C_{(p,r)} + C_{(p,q)} = C_{(p,q)} + C_{(p,r)}$

TABLE 2.8. Coefficient relations of Theorem 2.2.1.

for all $p, q, r \neq 0$. Combining the second and third relation gives that $C_{(\sigma^l(a),\sigma^m(b))} = C_{(a,b)}$ for all l, m and $a, b \neq 0$. Therefore, $C_{(a,b)} = C_{(c,d)}$ whenever $orb(a) = orb(c)$ and $orb(b) = orb(d)$.

Consider the coboundaries of $C^1_Q(P^\sigma_n; A)$'s generators χ_m. If $m = 0$,

$$\delta\chi_0(x_0, x_1) = \chi_0(x_0) - \chi_0(x_0 * x_1) = 0.$$

If $m \neq 0$,

$$\delta\chi_m(x_0, x_1) = \chi_m(x_0) - \chi_m(x_0 * x_1) = \chi_{(m,0)} - \chi_{(\sigma^{-1}(m),0)}.$$

Therefore, $\chi_{(p,0)}$ is cohomologous to $\chi_{(q,0)}$ whenever $orb_\sigma(p) = orb_\sigma(q)$. Let m_1, m_2, ..., m_k represent the cycles of σ. The relations and coboundary information give that ϕ is cohomologous to

$$\sum_{j=1}^{k} \left[C_{(0,m_j)} \left(\sum_{i \in orb_\sigma(m_j)} \chi_{(0,i)} \right) \right] + \sum_{j=1}^{k} \left[\left(\sum_{i \in orb_\sigma(m_j)} C_{(i,0)} \right) \chi_{(m_j,0)} \right] + \sum_{j,h=1, j \neq h}^{k} \left[C_{(m_j,m_h)} \left(\sum_{i \in orb_\sigma(m_j)} \sum_{t \in orb_\sigma(m_h)} \chi_{(i,t)} \right) \right],$$

showing that the second homology group is free on $2k$ plus $k * (k-1)$ generators.

□

The following theorem characterizes P^σ_n's good involutions. This will be used to calculate a second symmetric quandle cohomology group of P_3.

THEOREM 2.2.2. *If σ is not an involution, then P_n^σ has no good involutions. If σ is a non-trivial involution, an involution ρ on P_n^σ is good if and only if $\rho(0) = 0$ and as a permutation on the positive integers $\rho \in C_{S_n}(\sigma)$.*

PROOF. Suppose that ρ is a good involution on P_n^σ with $\rho(0) \neq 0$. Then, $x = x * \rho(0) = x \,\overline{*}\, 0 = \sigma^{-1}(x)$ for all $x \neq 0$ implying that $\sigma = id$. Therefore, $\rho(0) = 0$ and $\sigma(x) = x * 0 = x * \rho(0) = x \,\overline{*}\, 0 = \sigma^{-1}(x)$ for all $x \neq 0$, i.e. σ is an involution. Since $\rho(\sigma(x)) = \rho(x * 0) = \rho(x) * 0 = \sigma(\rho(x))$ for all $x \neq 0$, ρ is in σ's centralizer.

Now suppose that ρ is an involution on P_n^σ fixing 0 and restricting to a permutation in the centralizer of σ. A case study shows that ρ is good, see Table 2.9.

x	y	$\rho(x * y) = \rho(x) * y$	$x * \rho(y) = x \,\overline{*}\, y$
$+$	$+$	$\rho(x) = \rho(x)$	$x = x$
$+$	0	$\rho(\sigma(x)) = \sigma(\rho(x))$	$\sigma(x) = \sigma^{-1}(x)$
0	$+$	$0 = 0$	$0 = 0$
0	0	$0 = 0$	$0 = 0$

TABLE 2.9. Verification that ρ is good.

□

THEOREM 2.2.3. *Let $\rho : P_3 \to P_3$ be the transposition* (12)*. Then,*

$$H^2_{Q,\rho}(P_3; \mathbb{Z}_2) = \mathbb{Z}_2.$$

PROOF. Theorem 2.2.1 shows that any cocycle $\sum_{i,j \in P_n^\sigma} C_{(i,j)}\chi_{(i,j)} \in Z^2_{Q,\rho}(P_3; \mathbb{Z}_2)$ is cohomologous to

$$C_{(0,1)}(\chi_{(0,1)} + \chi_{(0,2)}) + (C_{(1,0)} + C_{(2,0)})\chi_{(1,0)}$$

in $H^2_{Q,\rho}(P_3; \mathbb{Z}_2)$. Since $2(0,1), (1,0)+(2,0) \in D_2^\rho$, the coefficients satisfy $2C_{(0,1)} = C_{(1,0)}+C_{(2,0)} = 0$. Thus,

$$\chi_{(0,1)} + \chi_{(0,2)}$$

represents a generator of the order 2 group $H^2_{Q,\rho}(P_3; \mathbb{Z}_2)$.

□

2.3. The Quiver and Cocycle Invariant of Links Using P_n^σ

In this section, the cocycle $\theta \in Z_Q^2(P_n^{n-cycle}; \langle t^k : k \in \mathbb{Z} \rangle)$ given by

$$\theta = t^{\sum_{i=1}^{n} \chi_{(0,i)}}$$

will be used to compute the cocycle invariant Φ_θ. This was shown to be a cocycle in Theorem 2.2.1. The cocycle takes the value t on any tuple of the form $(0, a)$ where a is positive. Quandle quivers $\mathcal{Q}_{P_n^\sigma}^S$ will be computed using an arbitrary permutation σ and $S \subseteq End(P_n^\sigma)$.

DEFINITION 2.3.1. *Let K_1 and K_2 be components of an oriented link. Figure 2.2 describes the 4 types of crossings between K_1 and K_2 where the horizontal arcs belong to K_1 and the vertical arcs belong to K_2. Let n_1, n_2, n_3, and n_4 denote the number of crossings of type (i), (ii), (iii), and (iv). The pairwise linking number between K_1 and K_2 is defined by*

$$lk(K_1, K_2) = \frac{n_1 + n_2 - n_3 - n_4}{2} = n_1 - n_4 = n_2 - n_3.$$

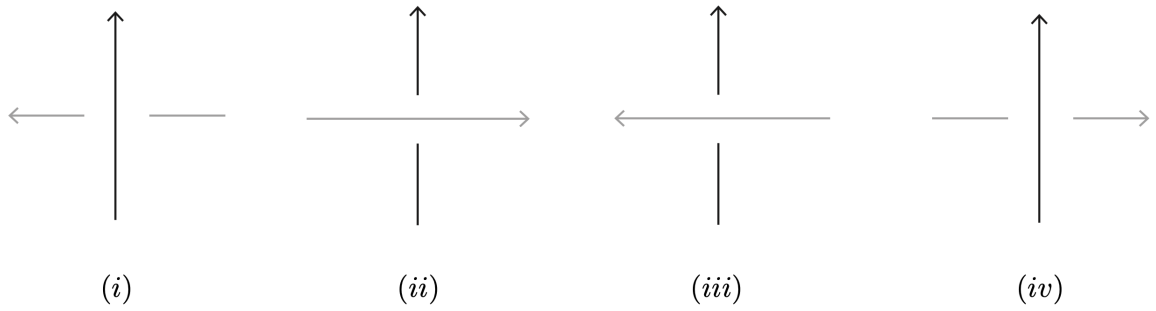

FIGURE 2.2. Crossing types between 2 components.

THEOREM 2.3.2. *The quiver $\mathcal{Q}_{P_n^\sigma}^S(L)$ of a 2-component link $L = K_1 \cup K_2$ is determined by $lk(K_1, K_2)$.*

PROOF. Let a_i be some arc of K_i. The trivial quandle embeds into P_n^σ and coloring L using this subquandle, the positive integers of P_n^σ, simplifies to independently selecting the colors of a_1 and a_2.

If a_1 is colored 0 then all arcs of K_1 are assigned 0 since $0 * x = 0$ for any $x \in P_n^\sigma$. If the arc a_2 is also colored 0, then the link is trivially colored. If a_2 is colored with a positive integer k, then k's

cycle length $|orb_\sigma(k)|$ must divide the linking number $lk(K_1, K_2)$. To see this, color the arcs of K_2 following an orientation and starting with a_2. When the arc meets a crossing as an under arc the other under arc must be colored k if the over strand is from K_2, $\sigma(k)$ if the over strand is from K_1 and the crossing is positive, and $\sigma^{-1}(k)$ if the over strand is from K_1 and the crossing is negative. Therefore, $\sigma^{lk(K_1,K_2)}(k) = k$ and $|orb_\sigma(k)|$ divides $lk(K_1, K_2)$.

Let T be the sum of σ's cycle lengths which divide $lk(K_1, K_2)$. When a_1 is colored 0 there are T choices of colors for a_2 that uniquely extend to non-trivial colorings of L. Likewise, there are T choices of colors for a_1 when a_2 is colored 0. The P_n^σ-colorings of L are parametrized by the colorings (x_1, x_2) of the arcs a_1 and a_2. The ordered pair (x_1, x_2) represents arc colors of a_1 and a_2 that uniquely extend to a P_n^σ-coloring of L if $x_1, x_2 \neq 0$, $x_1 = 0$ and $|orb_\sigma(x_2)|$ divides $lk(K_1, K_2)$, $x_2 = 0$ and $|orb_\sigma(x_1)|$ divides $lk(K_1, K_2)$, or $x_1 = x_2 = 0$. The action of $End(P_n^\sigma)$ on $Col_{P_n^\sigma}(L)$ is determined by its action on the ordered pairs (x_1, x_2) representing colorings. Therefore, the linking number $lk(K_1, K_2)$ determines the quiver $\mathcal{Q}^S_{P_n^\sigma}(K_1 \cup K_2)$.

□

COROLLARY 2.3.1. *The quandle cocycle invariant Φ_θ of a 2-component link $L = K_1 \cup K_2$ is determined by $lk(K_1, K_2)$.*

PROOF. Suppose that (x_1, x_2) represents a P_n^σ-coloring of L where σ is an n-cycle. The θ-weight of L with respect to (x_1, x_2) is 0 when $x_1 = x_2 = 0$ or $x_1, x_2 \neq 0$. If $x_2 \neq x_1 = 0$, then the corresponding θ-weight is $t^{lk(K_1,K_2)}$. To see this, let K_1 represent the horizontal component and let K_2 represent the vertical component in Figure 2.2. Then the crossing types (i), (ii), (iii), and (iv) have θ-weights t, 0, 0, and t^{-1}. Since the number of (i) crossings minus the number of (iv) crossings equals the linking number, the corresponding θ-weight of the coloring is $t^{lk(K_1,K_2)}$. Likewise, the θ-weight when $x_1 \neq x_2 = 0$ is $t^{lk(K_1,K_2)}$. This also holds if K_1 represented the vertical component and K_2 represented the horizontal component in Figure 2.2.

If n divides the linking number, then there are $2n$ colorings with a θ-weight of $t^{lk(K_1,K_2)}$,

$$(0,1), (0,2), \ldots, (0,n), (1,0), (2,0), \ldots, (n,0).$$

In this case, $\Phi_\theta(L) = 1 + n^m + 2nt^{lk(K_1,K_2)}$. When n does not divide the linking number, $\Phi_\theta(L) = 1 + n^m$.

□

DEFINITION 2.3.3. *The linking graph of a link L is a complete graph with vertices representing L's components and edge weights representing the linking numbers between components.*

LEMMA 2.3.3.1. *Every complete, simple graph with integral weights represents the linking graph of some link.*

PROOF. Let G be a complete graph on n vertices with integral weights. Take n points equidistant along the unit circle. The graph G is represented by connecting each pair of points with a line segment. Assume after a small perturbation that any two arcs intersect transversally in double points along their interiors or not at all. Give these double points arbitrary crossing information. Take small disk neighborhoods of the vertices missing the crossings then remove the interiors of the disks. This leaves a 3-valent, singular link diagram seen as edges connecting unknotted circles, Figure 2.3. Replace a small neighborhood of the edges with the tangle in Figure 2.4 such that the number of twists equals the weight of the edge that it is replacing. Arbitrarily orient the components and replace any twist region with its mirror if the sign of its crossings does not equal the sign of the weight that it replaced. This gives an oriented link whose linking graph is G.

□

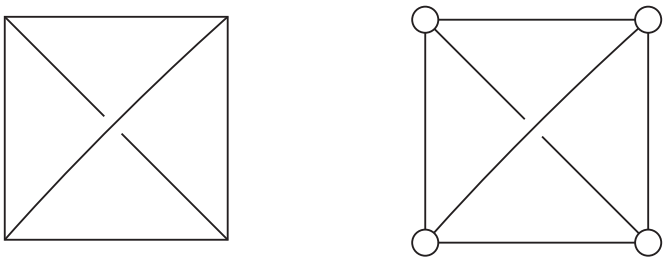

FIGURE 2.3. Removing the interiors of disk neighborhoods.

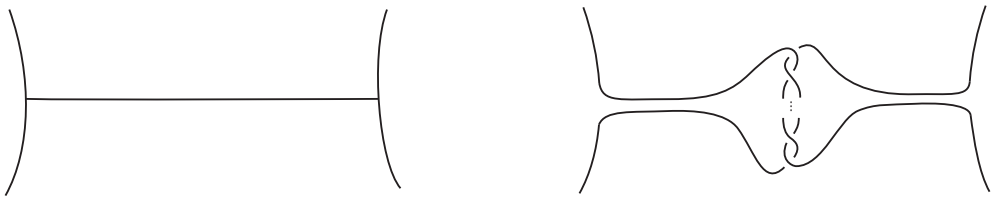

FIGURE 2.4. Replacing an edge with a twist tangle.

THEOREM 2.3.4. *If two links have isomorphic linking graphs, then they have isomorphic quivers* $\mathcal{Q}^S_{P^\sigma_n}$ *and equal cocycle* Φ_θ *invariants.*

PROOF. Let $L = K_1 \cup \cdots \cup K_m$ be a diagram of an m-component link. Let a_i be some arc of K_i. The P^σ_n-colorings of L can be parametrized by the m-tuple of colors $(x_1, \ldots, x_m)$ assigned to $a_1, \ldots, a_m$. An m-tuple of colors $(x_1, \ldots, x_m) \in (P^\sigma_n)^m$ represents the colors of the arcs $(a_1, \ldots, a_m)$ in a P^σ_n-colorings of L if and only if whenever $x_i = 0$, $|orb_\sigma(x_j)|$ divides $lk(K_i, K_j)$ for all $x_j \neq 0$. The action of $End(P^\sigma_n)$ on $Col_{P^\sigma_n}(L)$ is determined by its action of the set of m-tuples $(x_1, \ldots, x_m)$ representing the colorings. Any other link with an isomorphic linking graph will produce the same set of m-tuples $(x_1, \ldots, x_m)$ up to a fixed permutation of the entries. Therefore, their quivers are equal.

If $x_i \neq x_j = 0$, then the θ-weight contributed by the crossings of K_i and K_j in the coloring $(x_1, \ldots, x_m)$ is $t^{lk(K_i,K_j)}$ as justified in Corollary 2.3.1. The θ-weight of a coloring $(x_1, \ldots, x_m)$ is

$$\sum_{i<j \ \wedge \ (x_i \neq x_j = 0 \ \vee \ 0 = x_i \neq x_j)} t^{lk(K_i,K_j)}.$$

Since the θ-weight of a coloring is determined by its representative m-tuple $(x_1, \ldots, x_m)$ and L's linking numbers, two links with isomorphic linking graphs will have equal cocycle invariants.

□

COROLLARY 2.3.2. *If two links have spanning trees in their linking graphs such that no cycle length of* σ *divides a weight in these trees, then their quivers* $\mathcal{Q}^S_{P^\sigma_n}$ *are isomorphic and their cocycle invariants* Φ_θ *equal* $1 + n^m$.

PROOF. Let L be an m-component link with $(x_1, \ldots, x_m) \in (P^\sigma_n)^m$ parametrizing its P^σ_n-colorings. As before, such an m-tuple represents a coloring if and only if whenever $x_i = 0$, $|orb_\sigma(x_j)|$ divides $lk(K_i, K_j)$ for all $x_j \neq 0$.

For any two components K_i and K_j of L consider the path in the spanning tree connecting them. This gives a sequence of components whose consecutive linking numbers are not divisible by any cycle length of σ. As such, if K_i is colored 0, i.e. $x_i = 0$, then each consecutive component in the sequence must also be colored 0, namely $x_j = 0$. Therefore, if any entry in $(x_1, \ldots, x_m)$ is zero, then all entries are zero.

In addition to the n^m colorings using the positive integers there is a trivial coloring assigning all arcs 0. Each coloring has a trivial θ-weight, so $\Phi_\theta(L) = 1 + n^m$. Since the action of $End(P_n^\sigma)$ on the tuples $(x_1, \ldots, x_m)$ determines the quiver $\mathcal{Q}^S_{P_n^\sigma}(L)$, any other link satisfying the spanning tree condition will have an isomorphic quiver and equal cocycle invariant Φ_θ.

□

COROLLARY 2.3.3. *Suppose that σ has no fixed points. The pairwise linking numbers of a link with more than 2 components do not determine its quiver $\mathcal{Q}^S_{P_n^\sigma}$ or cocycle invariant Φ_θ.*

PROOF. Take any spanning tree in a complete, simple graph and give all edges a weight of 1. Weight all but one of the remaining edges 1. There are infinitely many choices for the remaining weight that give non-isotopic links with isomorphic quivers and equal cocycle invariants.

□

CHAPTER 3

Surface-link Families with Arbitrarily Large Triple Point Number

Satoh and Shima proved many foundational results on the triple point number in the early 2000's:

THEOREM 3.0.1 (Satoh '00 [54]). *No surface-knot has a triple point number of 1.*

THEOREM 3.0.2 (Satoh '01 [55]). *For any positive n, there exists a surface-knot whose triple point number is $2n$.*

THEOREM 3.0.3 (Satoh-Shima '03 [59]). *The 2-twist-spun trefoil has a triple point number of 4.*

THEOREM 3.0.4 (Satoh-Shima '05 [60]). *The 3-twist-spun trefoil has a triple point number of 6.*

THEOREM 3.0.5 (Satoh '05 [56]). *No 2-knot has a triple point number of 2 or 3.*

Hatakenaka generalized the method used to compute the triple point number of the 2-twist-spun trefoil to show that the triple point number of the 2-twist-spun figure eight knot is between 6 and 8 and the triple point number of the 2-twist-spun (2,5)-torus knot is between 6 and 12 [31]. Satoh then returned to the problem to calculate these surface-knots' exact triple point number:

THEOREM 3.0.6 (Satoh '16 [58]). *The 2-twist-spun figure-eight knot and the 2-twist-spun (2,5)-torus knot have a triple point number of 8.*

It is known that no surface-knot of genus one has a triple point number of 2 [1]. Currently, the only examples of surface-knots with triple point number of two are non-orientable surface-links. The only calculated triple point numbers have been even, although there are too few examples to suggest that the triple point number must always be even.

There are few infinite families of surface-knots with calculated or bounded triple point numbers. Kamada provided the first result of the kind:

THEOREM 3.0.7 (Kamada '93 [36]). *For any positive integer n, there exists some 2-knot S such that $t(S) > n$.*

Kamada's algebraic proof allows for the addition of trivial handles to generalize the result to connected, orientable surface-knots of any genus.

In 2001, Satoh showed that non-split 2-component surface-links whose components are trivial, non-orientable, and of arbitrary genus can achieve arbitrarily large triple point number [55]. His lower bound calculation relies on each component being non-orientable, P^2-irreducible, and having nonzero normal Euler number. In 2009, Kamada and Oshiro showed a similar result using symmetric quandles [40]. In 2010, Oshiro further explored their method to show that there are non-split 2-component surface-links with both components trivial and non-orientable whose triple point number can be made arbitrarily large regardless of normal Euler number [51].

Theorem 3.0.8 generalizes Oshiro's family and calculation by adding trivial components and extending the original quandle coloring:

THEOREM 3.0.8. *For any non-negative integers k and m, there exists a non-split $k+m+1$-component surface-link $F = \cup_{i=1}^{k} F_i \cup \cup_{i=1}^{m} F_i' \cup G$ such that*

(i) F_i is trivial and orientable of arbitrary genus g_i,

(ii) F_i' is trivial and non-orientable of arbitrary even genus g_i',

(iii) G is trivial and orientable of genus $m+k$,

(iv) $F - G$ is a trivial surface-link,

(v) $t(F) = \sum_{i=1}^{m} g_i'$.

Section 3.1 provides background information on the weight of symmetric quandle 3-cocycles, Section 3.2 describes the induced broken sheet diagram of a motion picture, and Section 3.3 proves Theorem 3.0.8.

3.1. The Weight of a Symmetric Quandle 3-cocycle

This section begins with some equivalent definitions for use in this chapter.

A *quandle* is a set X with a binary operation $(x, y) \mapsto x^y$ such that

(i) for any $x \in X$, it holds that $x^x = x$,

(ii) for any $x, y \in X$, there exists a unique $z \in X$ such that $z^y = x$, and

(iii) for any $x, y, z \in X$, it holds that $(x^y)^z = (x^z)^{(y^z)}$.

For a quandle X, a *good involution* ρ *of* X is an involution such that

(i) for any $x, y \in X$, $\rho(x^y) = \rho(x)^y$, and

(ii) for any $x, y \in X$, $x^{\rho(y)} = x^{y^{-1}}$.

A quandle paired with a good involution is called a *symmetric quandle*.

Let (X, ρ) be a symmetric quandle and A an abelian group. A homomorphism $\phi : \mathbb{Z}(X^3) \to A$ is a *symmetric quandle 3-cocyle of* (X, ρ) if the following conditions are satisfied:

(i) For any $(a, b, c, d) \in X^4$,

$$\phi(a, c, d) - \phi(a^b, c, d) - \phi(a, b, d) + \phi(a^c, b^c, d) + \phi(a, b, c) - \phi(a^d, b^d, c^d) = 0,$$

(ii) for any $(a, b) \in X^2$, $\phi(a, a, b) = 0$ and $\phi(a, b, b) = 0$, and

(iii) for any $(a, b, c) \in X^3$,

$$\phi(a, b, c) + \phi(\rho(a), b, c) = 0,$$

$$\phi(a, b, c) + \phi(a^b, \rho(b), c) = 0,$$

$$\text{and} \quad \phi(a, b, c) + \phi(a^c, b^c, \rho(c)) = 0.$$

For any symmetric quandle (X, ρ), there is an associated chain and cochain complex. Symmetric quandle 3-cocycles are cocycles of this cochain complex and represent cohomology classes of $H^3_{Q,\rho}(X; A)$, see [11], [38], [40].

Let L be a classical link diagram. Divide over-arcs at each crossing to produce the *semi-arcs* of L. For a symmetric quandle (X, ρ), an assignment of a normal orientation and X elements to each semi-arc satisfies the *coloring conditions* if the following hold:

(i) Suppose that the two adjacent semi-arcs coming from an over-arc at a crossing of L are labeled with X elements x_1 and x_2. If the normal orientations are coherent then $x_1 = x_2$, otherwise $x_1 = \rho(x_2)$. See the top row of Figure 3.1.

(ii) Suppose that the two under-arcs at a crossing are labeled with X elements x_1 and x_2, and that one of the semi-arcs coming from the over-arc is labeled x_3 with a normal orientation pointing toward the under-arc labeled with x_2. If the normal orientations of the under-arcs are coherent, then $x_1^{x_3} = x_2$, otherwise $x_1^{x_3} = \rho(x_2)$. See the bottom row of Figure 3.1.

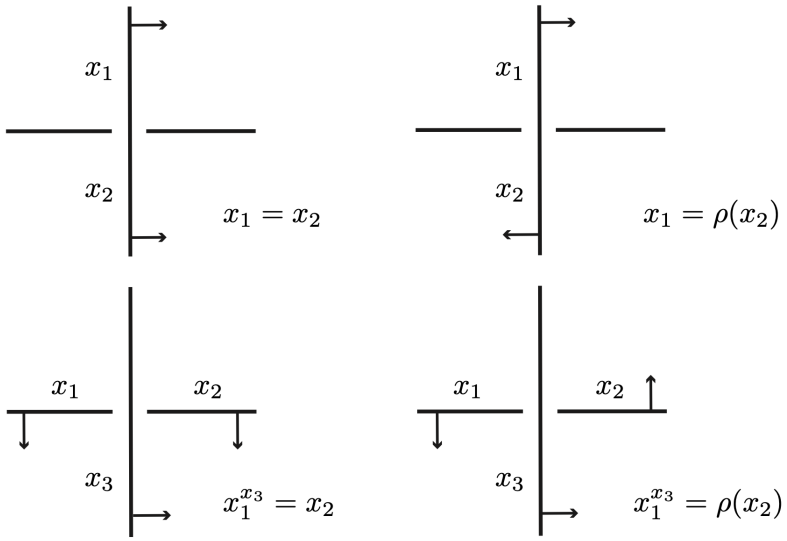

FIGURE 3.1. Coloring conditions of a link diagram.

An (X, ρ)-*coloring* of L is the equivalence class of an assignment of normal orientations and elements of X to the semi-arcs of L satisfying the coloring conditions. The equivalence relation is generated by *basic inversions*. Such an inversion reverses the normal orientation of a semi-arc and changes the assigned element x to $\rho(x)$.

Let D be a broken sheet diagram. Divide over-sheets along the double point curves and call the result *semi-sheets* of D. Note that every semi-sheet is orientable even if F is non-orientable. For a symmetric quandle (X, ρ), an assignment of a normal orientation and an element of X to each semi-sheet satisfies the *coloring conditions* if the following hold:

(i) Suppose that two adjacent semi-sheets coming from an over-sheet of D about a double point curve are labeled by x_1 and x_2. If the normal orientations are coherent then $x_1 = x_2$, otherwise $x_1 = \rho(x_2)$. See the top row of Figure 3.2.

(ii) Suppose that two adjacent semi-sheets S_1 and S_2 coming from under-sheets about a double point curve are labeled by x_1 and x_2, and that one of the two semi-sheets coming from an over-sheet of D, say S_3, is labeled by x_3. Assume that the normal orientation of S_3 points from S_1 to S_2. If the normal orientations of S_1 and S_2 are coherent, then $x_1^{x_3} = x_2$, otherwise $x_1^{x_3} = \rho(x_2)$. See the bottom row of Figure 3.2.

An (X, ρ)-*coloring* of D is the equivalence class of an assignment of normal orientations and elements of X to the semi-sheets of D satisfying the coloring conditions. The equivalence relation

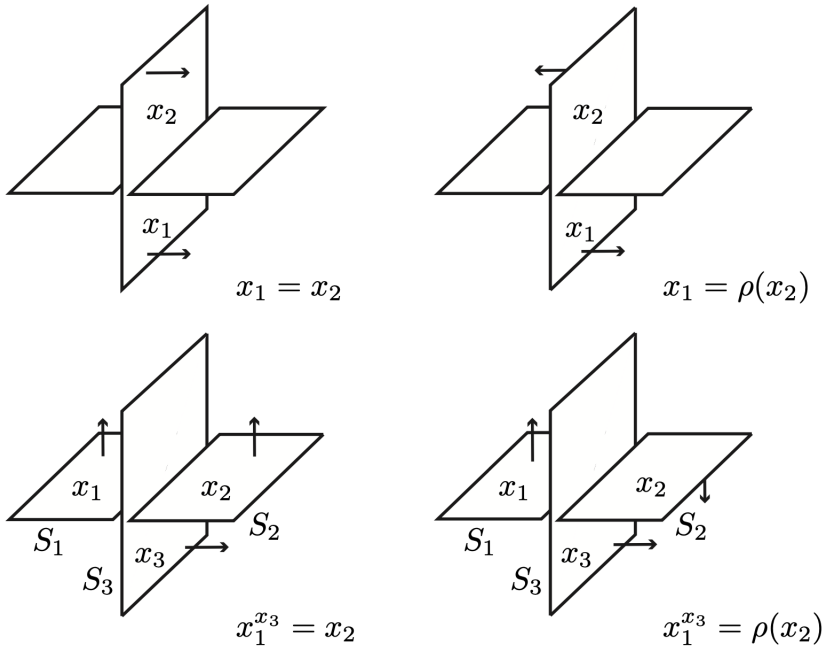

FIGURE 3.2. Coloring conditions of a broken sheet diagram.

is generated by *basic inversions*. Such an inversion reverses the normal orientations of a semi-sheet and changes the assigned element x to $\rho(x)$ [40], [51].

Let C be an (X, ρ)-coloring of a broken sheet diagram D. For a triple point τ of D, choose one of the eight 3-dimensional complementary regions around the triple point and call the region *specified*. There are 12 semi-sheets around a triple point. Let S_B, S_M, and S_T be the three of them that face the specified region, where S_B, S_M, and S_T are semi-sheets of the bottom, middle, and top sheet respectively. Let n_B, n_M, and n_T be the normal orientations of S_B, S_M, and S_T. Through basic inversions, it is assumed that each normal orientation points away from the specified region. Let x, y, and z be the elements of X assigned to the semi-sheets S_B, S_M, and S_T whose normal orientations n_B, n_M, and n_T point away from the specified region. The *color* of the triple point τ is the triple $C_\tau = (x, y, z)$.

Let $\phi : \mathbb{Z}(X^3) \to A$ be a symmetric quandle 3-cocycle of (X, ρ). The $\phi - weight$ of the triple point is defined by $\epsilon\phi(x, y, z)$ such that ϵ is +1 (or -1) if the triple of the normal orientations (n_T, n_M, n_B) is (or is not) coherent with the orientation of $\mathbb{R}^3$ at the triple point. The triple point of Figure 3.3 is positive. The $\phi - weight$ of a diagram D with respect to a symmetric quandle

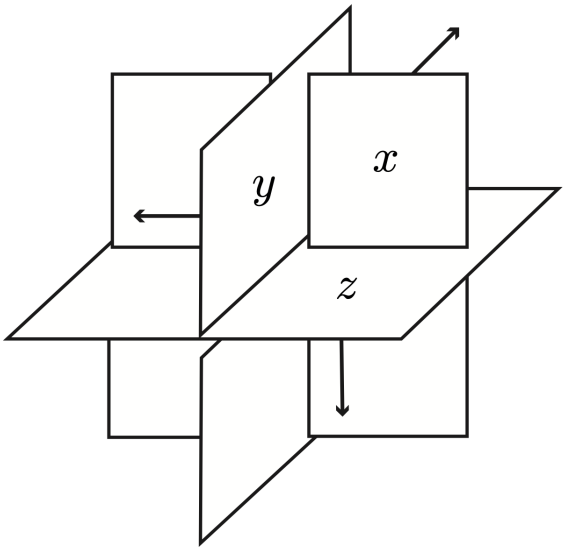

FIGURE 3.3. A positive colored triple point with $C_\tau = (x, y, z)$.

coloring C is

$$\phi(D, C) = \sum_{\tau} (\phi - \text{weight of } \tau) \in A,$$

where τ runs over all triple points of D. The value $\phi(D, C)$ is an invariant of an (X, ρ)-colored surface-link (F, C) [40, 51]. Denote $\phi(D, C)$ by $\phi(F, C)$.

3.2. Induced Broken Sheet Diagram of a Motion Picture

Given a surface-knot $F \subset \mathbb{R}^4$ and a vector $\mathbf{v} \in \mathbb{R}^4$, perturb F such that the orthogonal projection of $\mathbb{R}^4$ onto $\mathbb{R}$ in the direction of $\mathbf{v}$ is a Morse function. For any $t \in \mathbb{R}$, let $\mathbb{R}^3_t$ denote the affine hyperplane orthogonal to $\mathbf{v}$ that contains the point $t\mathbf{v}$. Morse theory allows for the assumption that all but finitely many of the non-empty cross-sections $F_t = \mathbb{R}^3_t \cap F$ are classical links. The decomposition $\{F_t\}_{t\in\mathbb{R}}$ is called a *motion picture* of F. It may also be assumed that the exceptional cross-sections contain minimal points, maximal points, and/or immersed links with double points representing saddles [10, 38].

There is a product structure between Morse critical points implying that only finitely many cross-sections are needed to decompose, or construct, F. Note that, a sole cross-section of a product region does not uniquely determine its knotting, ambient isotopy class relative boundary, see [10]. Project the cross-sections $\{F_t\}_{t\in\mathbb{R}}$ onto a plane to get an ordered family of planar diagrams containing classical link diagrams, minimal points, maximal points, and link diagrams with transverse

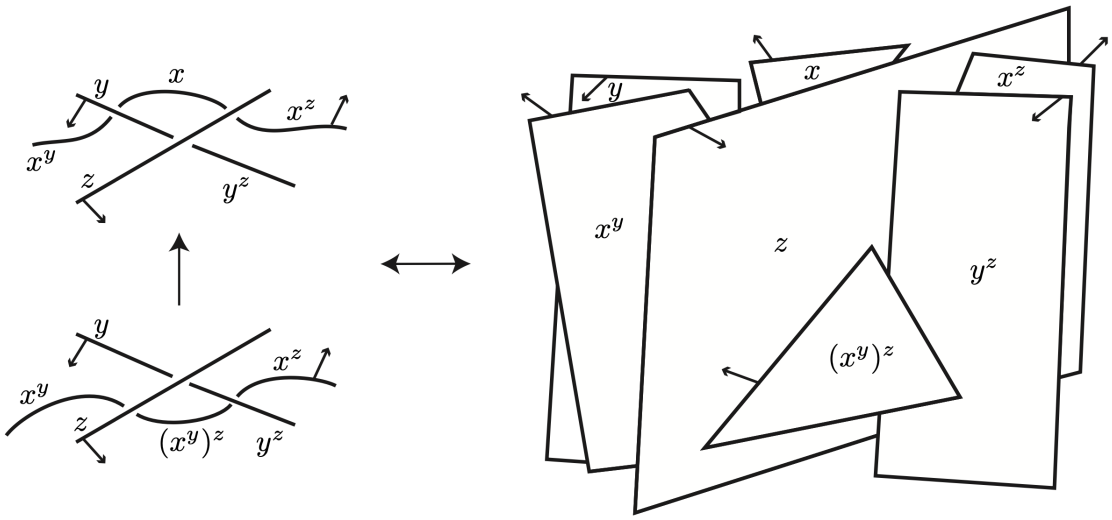

FIGURE 3.4. Relationship between Reidemeister III moves and triple points.

double points. These planar diagrams are *stills* of the motions picture. The collection of all stills will also be referred to as a motion picture. The double points of the immersed link diagrams can be replaced with bands to give information about the double points' smoothings in the stills immediately before and after.

FIGURE 3.5. Orientation at a saddle point.

The product structure between critical points also implies that cross-sections between consecutive critical points represent the same link. Therefore, there is a sequence of Reidemeister moves and planar isotopies between the stills of a motion picture that exists between consecutive critical points.

A motion picture induces a broken sheet diagram. Associate the time parameter of a Reidemeister move with the height of a local broken sheet diagram. A translation of each Reidemeister move to a broken sheet diagram is done in [39]. A Reidemeister III move gives a triple point diagram

seen in Figure 3.4, a Reidemeister I move corresponds to a branch point, and a Reidemeister II move corresponds to a maximum or minimum of a double point curve, Figures 5 & 6 of [39]. The triple points of the induced broken sheet diagram are in correspondence with the Reidemeister III moves between stills.

For a symmetric quandle (X, ρ), an (X, ρ)-coloring of an immersed link diagram with transverse double points is an assignment of X elements to each arc such that the symmetric coloring conditions are satisfied at each crossing, each of the four arcs at a double point are given the same color, and the normal orientations of the arcs at a double point satisfy Figure 3.5. Geometric justification of the coloring constraints at a double point, as well as an example of replacing a double point with a band, is shown in Figure 3.6.

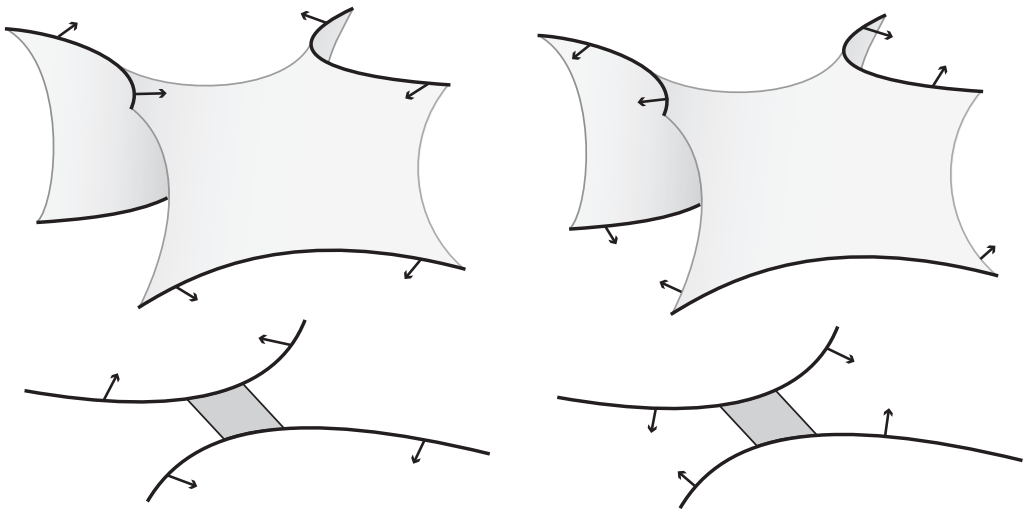

FIGURE 3.6. Induced saddle sheet.

An (X, ρ)-coloring of a motion picture is a *consistent* (X, ρ)-coloring of each still. Consistent means that stills separated by a Reidemeister move, or planar isotopy, have colorings consistent with the unique coloring extension of the move. An (X, ρ)-coloring of a motion picture gives an (X, ρ)-coloring of the induced broken sheet diagram. Give each induced sheet the same color as any arc that traces the sheet in the motion picture. With the addition of the appropriately colored saddle sheets, an (X, ρ)-coloring of the entire broken sheet diagram is achieved.

3.3. A Surface-link Family with Arbitrarily Large Triple Point Number

For non-negative integers s and t, let $A_{s,t}$ denote the direct sum of s copies of $\mathbb{Z}_2$ and t copies of $\mathbb{Z}$, $A_{s,t} = (\mathbb{Z}_2)^s \oplus (\mathbb{Z})^t$. Every element of $A_{s,t}$ is of the form $(\alpha_1 \oplus \cdots \oplus \alpha_s) \oplus (\beta_1 \oplus \cdots \oplus \beta_t)$, where α_i is an entry of the ith copy of $\mathbb{Z}_2$ and β_j is an entry of the jth copy of $\mathbb{Z}$. Let p_i and q_j be the elements of $A_{s,t}$ whose entries are all zeros except $\alpha_i = 1$ and $\beta_j = 1$.

Consider a broken sheet diagram realizing the triple point number of the surface-knot it represents. If a symmetric quandle 3-cocycle has $\mathbb{Z}$ coefficients and only takes the values $1, -1$ or 0, then the absolute value of the cocycle's weight cannot be greater than the number of triple points in the diagram. Since the weight of a symmetric quandle 3-cocycle is an invariant, the triple point number bounds the weight of the cocycle. This is the principle behind the following lemma.

LEMMA 3.3.0.1 (Oshiro '10 [51]). *Let (X, ρ) be a symmetric quandle, and let $\phi : \mathbb{Z}(X^3) \to A_{s,t}$ be a 3-cocycle of (X, ρ) such that for any generator $(a, b, c) \in X^3$ of $\mathbb{Z}(X^3)$ it holds that*

$$\phi(a, b, c) \in \{0, p_i, \pm q_j\}.$$

If the invariant $\phi(F, C)$ of a surface-knot F with an (X, ρ)-coloring C is equal to $(\alpha_1 \oplus \cdots \oplus \alpha_s) \oplus (\beta_1 \oplus \cdots \oplus \beta_t)$, then we have $t(F) \geq \sum_{i=1}^{s} \alpha_i + \sum_{i=1}^{t} |\beta_j|$ where the sum is taken in $\mathbb{Z}$ by regarding $\alpha_k = 0$ or 1 as an element of $\mathbb{Z}$.

Let P_3 be the quandle whose multiplication table is shown in Table 5.1. The involution $\rho : P_3 \to P_3$ defined by $\rho(0) = 0$ and $\rho(1) = 2$ is a good involution of P_3 [51].

P_3	0	1	2
0	0	0	0
1	2	1	1
2	1	2	2

TABLE 3.1. Multiplication table of P_3.

Define a map $\theta : P_3^3 \to \mathbb{Z}_2 \oplus \mathbb{Z}$ such that

$$\theta(a,b,c) = \begin{cases} 1 \oplus 0 & (a,b,c) \in \{(0,1,0),(0,2,0)\}, \\ 0 \oplus 1 & (a,b,c) \in \{(1,0,2),(2,0,1)\}, \\ 0 \oplus -1 & (a,b,c) \in \{(1,0,1),(2,0,2)\}, \\ 0 \oplus 0 & \text{otherwise.} \end{cases}$$

The linear extension $\theta : \mathbb{Z}(P_3^3) \to \mathbb{Z}_2 \oplus \mathbb{Z}$ is a symmetric quandle 3-cocycle of (P_3, ρ) [51]. This cocycle satisfies the assumptions of Lemma 5.4.2.1, so the θ-weight of a (P_3, ρ)-colored broken sheet diagram is a lower bound on the surface-knot's triple point number.

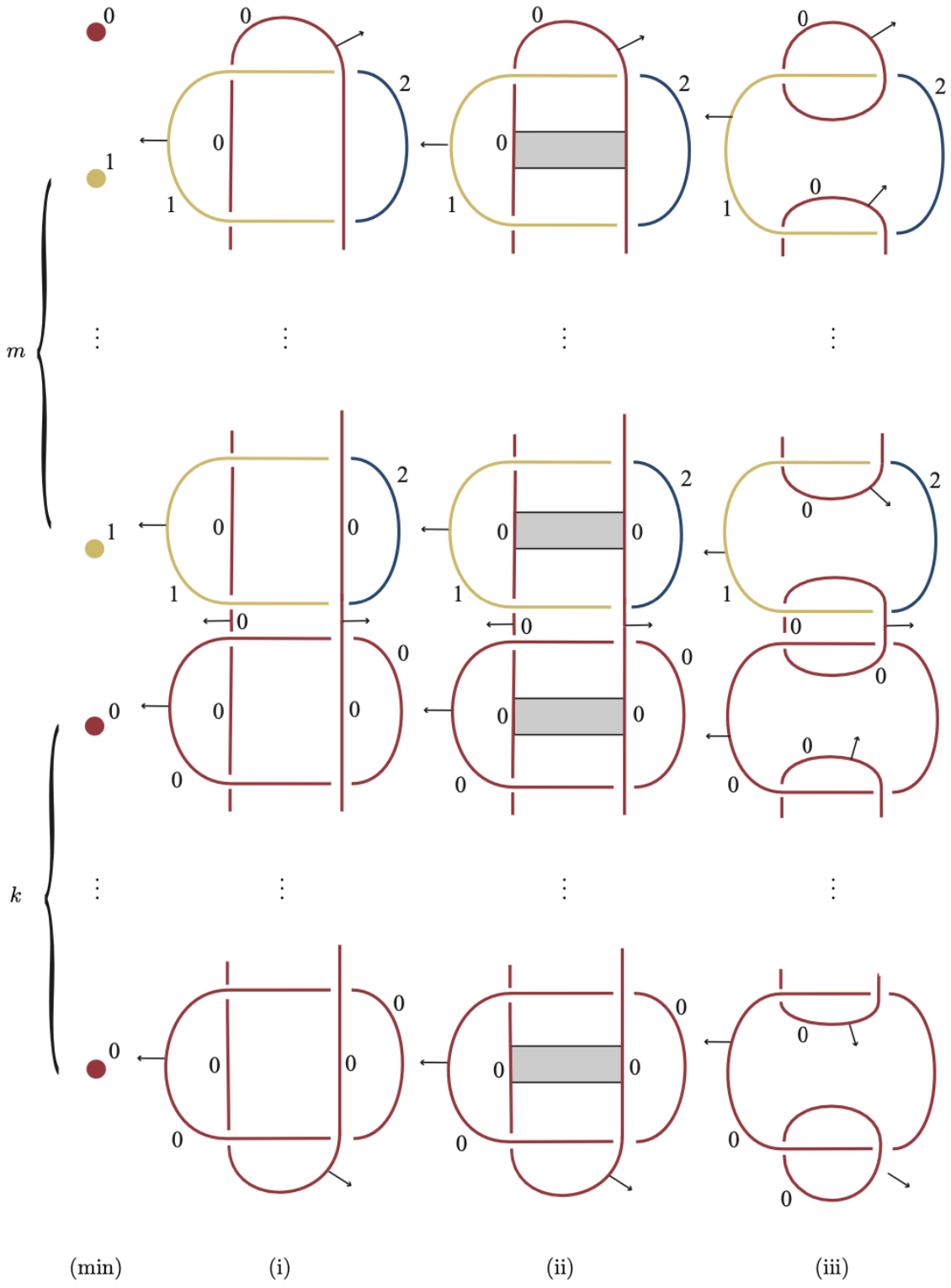

FIGURE 3.7. (P_3, ρ)-colored motion picture of F, 1 of 5.

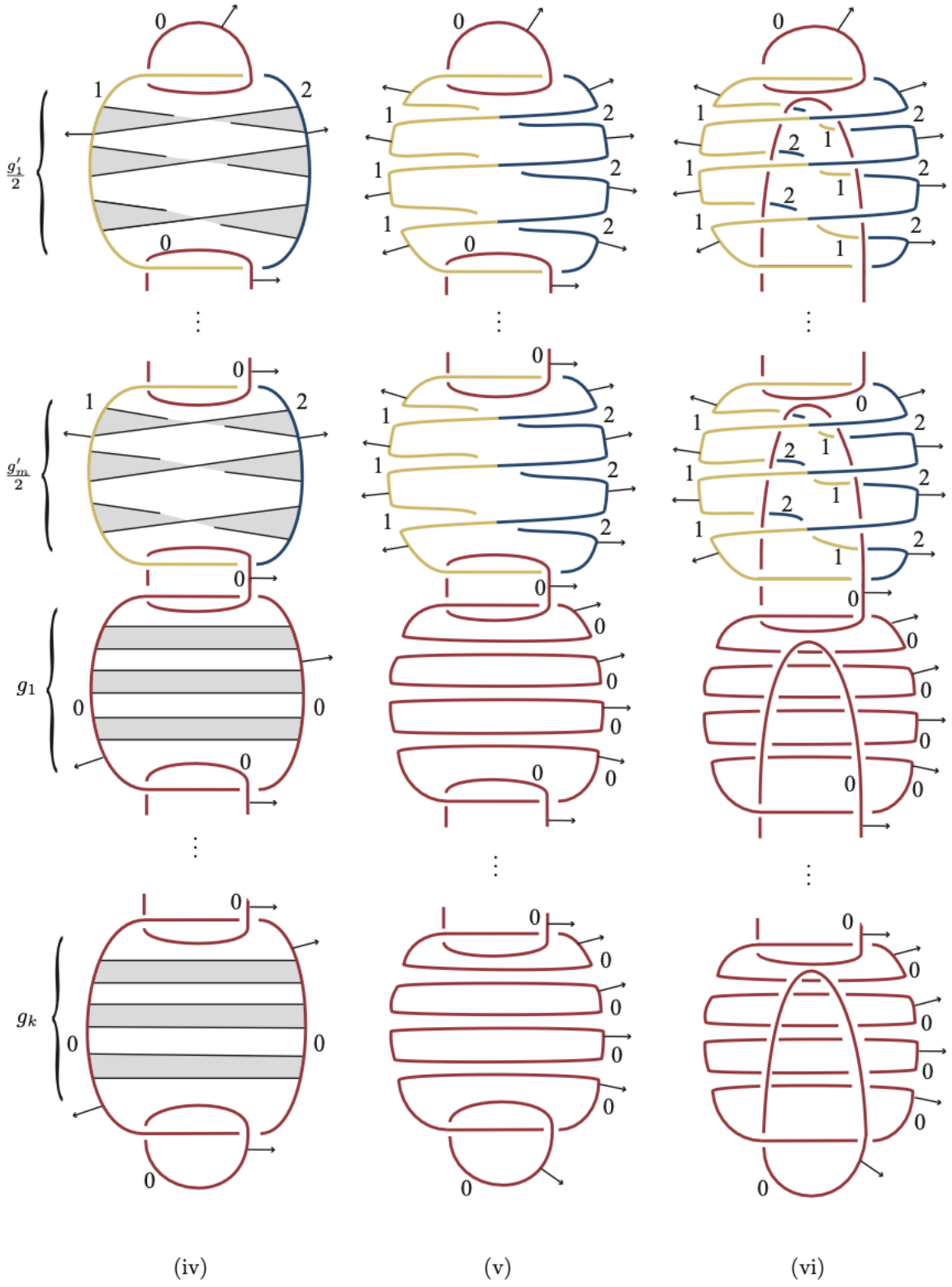

FIGURE 3.8. (P_3, ρ)-colored motion picture of F, 2 of 5.

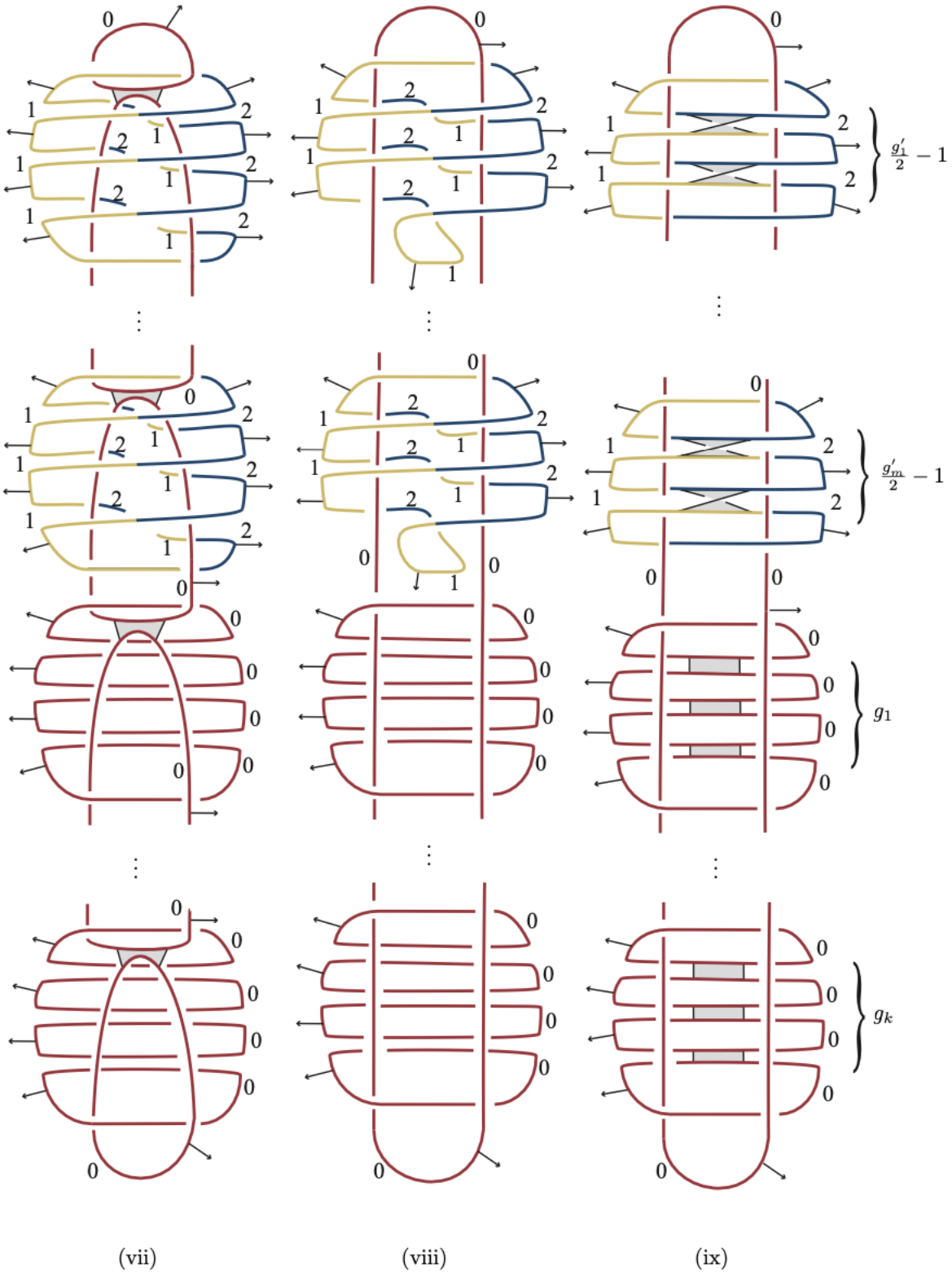

FIGURE 3.9. (P_3, ρ)-colored motion picture of F, 3 of 5.

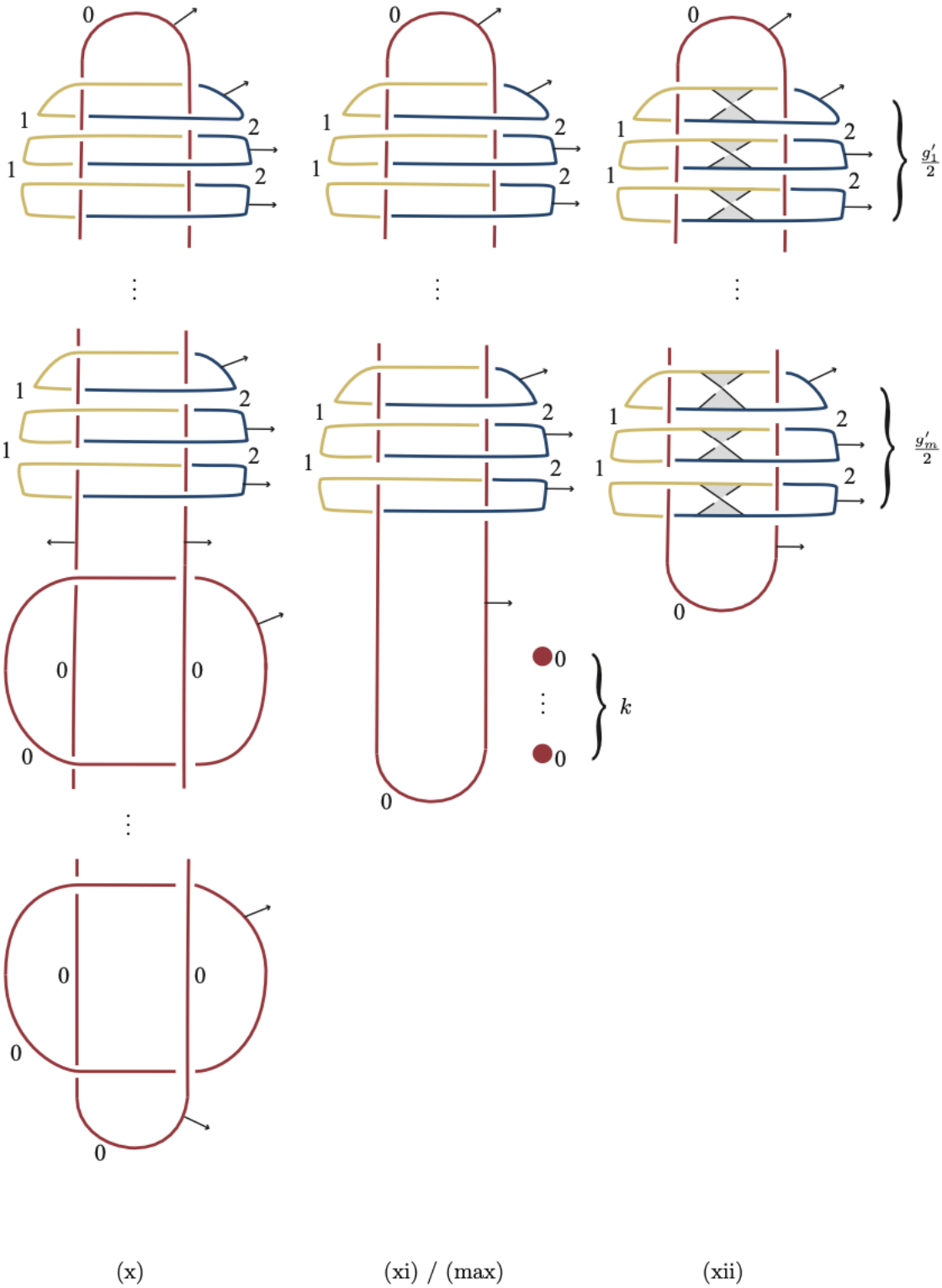

FIGURE 3.10. (P_3, ρ)-colored motion picture of F, 4 of 5.

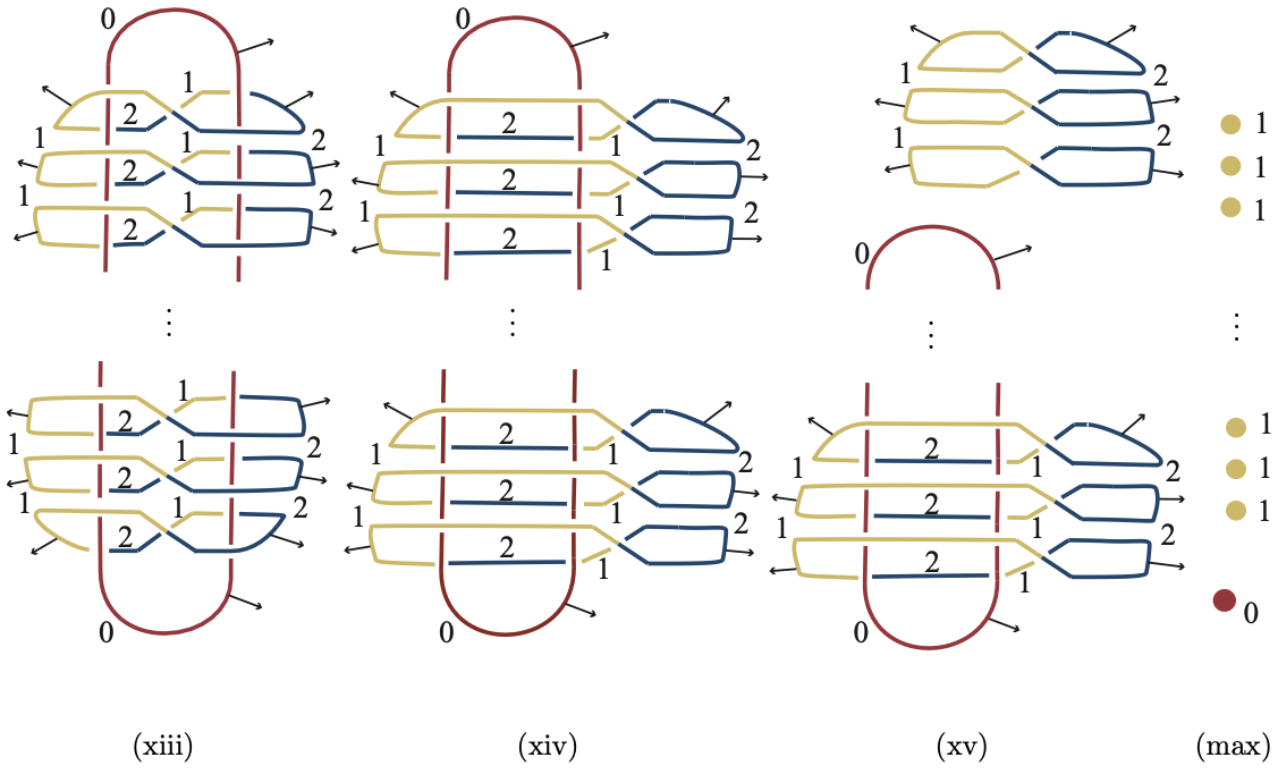

FIGURE 3.11. (P_3, ρ)-colored motion picture of F, 5 of 5.

PROOF OF THEOREM 3.0.8. Let F be the surface-link whose motion picture is shown in Figures 3.7, 3.8, 3.9, 3.10, and 3.11. This motion picture is (P_3, ρ)-colored. The first still shows the sole minimum of each component. There are m non-orientable components F_i', k orientable components F_i, and one component G such that $\cup_{i=1}^{m} F_i' \cup \cup_{i=1}^{k} F_i$ is a trivial surface-link.

There are $2(k+m)$ saddle points, one minimum, and one maximum in the motion picture restricted to G. Therefore, the trivial orientable surface-knot G has genus $k+m$. For any non-negative g_i, there are g_i saddle points of F_i in still (iv) and g_i in still (ix). Each F_i has a sole maximum, shown in still (xi). Therefore, F_i has genus g_i and bounds an obvious handlebody. For any positive even g_i', there are $\frac{g_i'}{2}$ saddle points of F_i' in still (iv), $\frac{g_i'}{2} - 1$ in still (ix), and $\frac{g_i'}{2}$ in still (xii). Since each F_i' has $\frac{g_i'}{2}$ maxima, F_i' has genus g_i'.

There are $\sum_{i=1}^{m} \frac{g_i'}{2}$ Reidemeister III moves between still (v) and (vi). These moves induce negative triple points each colored $(2, 0, 2)$. The sum of their θ-weights is $0 \oplus \sum_{i=1}^{m} \frac{g_i'}{2}$. Between still (xiii) and (xiv), there are $\sum_{i=1}^{m} \frac{g_i'}{2}$ Reidemeister III moves giving positive triple points each

colored $(1, 0, 2)$. The θ-weight sum of these triple points is $0 \oplus \sum_{i=1}^{m} \frac{g_i'}{2}$. Therefore, the θ-weight of the induced broken sheet diagram is $0 \oplus \sum_{i=1}^{m} g_i'$, and Lemma 5.4.2.1 implies that $t(F = \cup_{i=1}^{k} F_i \cup \cup_{i=1}^{m} F_i' \cup G) = \sum_{i=1}^{m} g_i'$ since the induced broken sheet diagram has $\sum_{i=1}^{m} g_i'$ triple points.

□

CHAPTER 4

On the Triple Point Number of Surface-links in Yoshikawa's Table

A *singular link diagram* is an immersed link diagram in the plane with crossings and transverse double points called *vertices*. At each vertex assign a *marker*, a local choice of two non-adjacent regions in the complement of the vertex. Such a marked singular link diagram is called a *ch-diagram* [10, 38, 39, 63]. One of the two smoothings of a vertex connects the two regions of the marker, the positive resolution L^+, and one separates the marker's regions, the negative resolution L^-, see Figure 4.1. If L^- and L^+ are unlinks, then the ch-diagram is said to be *admissible*. Admissible ch-diagrams represent surface-links and induce broken sheet diagrams, this is described in Section 5.1, and every surface-link defines an admissible ch-diagram.

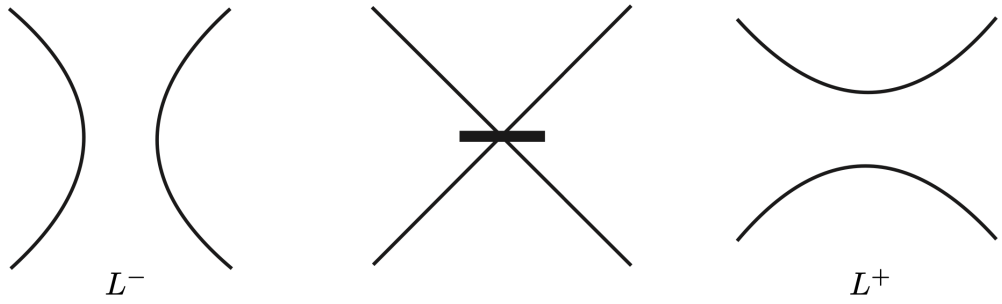

FIGURE 4.1. Smoothings of a marked vertex.

Including the 3 Reidemeister moves of classical link diagrams, there are 8 moves on ch-diagrams called *Yoshikawa moves*, see p.61 of [38]. Two admissible ch-diagrams represent equivalent surface-links if and only if they are Yoshikawa move equivalent, Theorem 3.6.3 of [38]. The ch-index of a ch-diagram is the number of marked vertices plus the number of crossings. The *ch-index* of a surface-link F, denoted $\mathrm{ch}(F)$, is the minimum of ch-indices $\mathrm{ch}(D)$ among all admissible ch-diagrams D representing F. A sufrace-link F is said to be *weakly prime* if F is not the connected sum of any two surfaces F_1 and F_2 such that $\mathrm{ch}(F_i) < \mathrm{ch}(F)$. Yoshikawa classified weakly prime surface-links whose ch-index is 10 or less in [63]. He generated a table of their representative ch-diagrams up to

orientation and mirror. A rendition of his table is done in Figure 4.2. His notation is of the form $I_k^{g_1,\ldots,g_c}$ where I is the surface-link's ch-index and $g_1,\ldots,g_c$ are the genera of its components.

This paper considers the triple point number of the surface-links represented in Yoshikawa's table. Section 5.2 tabulates the known triple point numbers of the surface-links from his table and calculates or provides bounds on the triple point number of the remaining surface-links.

4.1. Induced Broken Sheet Diagrams of Admissible Ch-diagrams

Material from Chapter 3 is repeated for clarity. Given a surface-knot $F \subset \mathbb{R}^4$ and a vector $\mathbf{v} \in \mathbb{R}^4$, perturb F so that the orthogonal projection of $\mathbb{R}^4$ onto $\mathbb{R}$ in the direction of $\mathbf{v}$ is a Morse function. For any $t \in \mathbb{R}$, let $\mathbb{R}^3_t$ denote the affine hyperplane orthogonal to $\mathbf{v}$ that contains the point $t\mathbf{v}$. Morse theory allows for the assumption that all but finitely many of the non-empty cross-sections $F_t = \mathbb{R}^3_t \cap F$ are classical links; the exceptional cross-sections contain minimal points, maximal points, and/or singular links. The decomposition $\{F_t\}_{t\in\mathbb{R}}$ is called a *motion picture* [23, 41].

There is a product structure between Morse critical points implying that only finitely many cross-sections are needed to decompose, or construct, F. Note that, a sole cross-section of a product region does not uniquely determine its knotting, i.e. its ambient isotopy class relative boundary, see [41]. Project the cross-sections $\{F_t\}_{t\in\mathbb{R}}$ onto a plane to get an ordered family of planar diagrams containing classical link diagrams, minimal points, maximal points, and singular link diagrams. These planar diagrams are *stills* of the motion picture. The collection of all stills is also referred to as a motion picture of the surface-link. The product structure between critical points implies that cross-sections between consecutive critical points represent the same link. Therefore, there is a sequence of Reidemeister moves and planar isotopies between the stills of a motion picture that exists between consecutive critical points. There is a translation of Reidemeister moves in a motion picture to sheets in a broken sheet diagram.

Associate the time parameter of a Reidemeister move with the height of a local broken sheet diagram. A Reidemeister III move gives a triple point diagram, a Reidemeister I move corresponds to a branch point, and a Reidemeister II move corresponds to a maximum or minimum of a double point curve, see Figure 4.8. Triple points of the induced broken sheet diagram are in correspondence

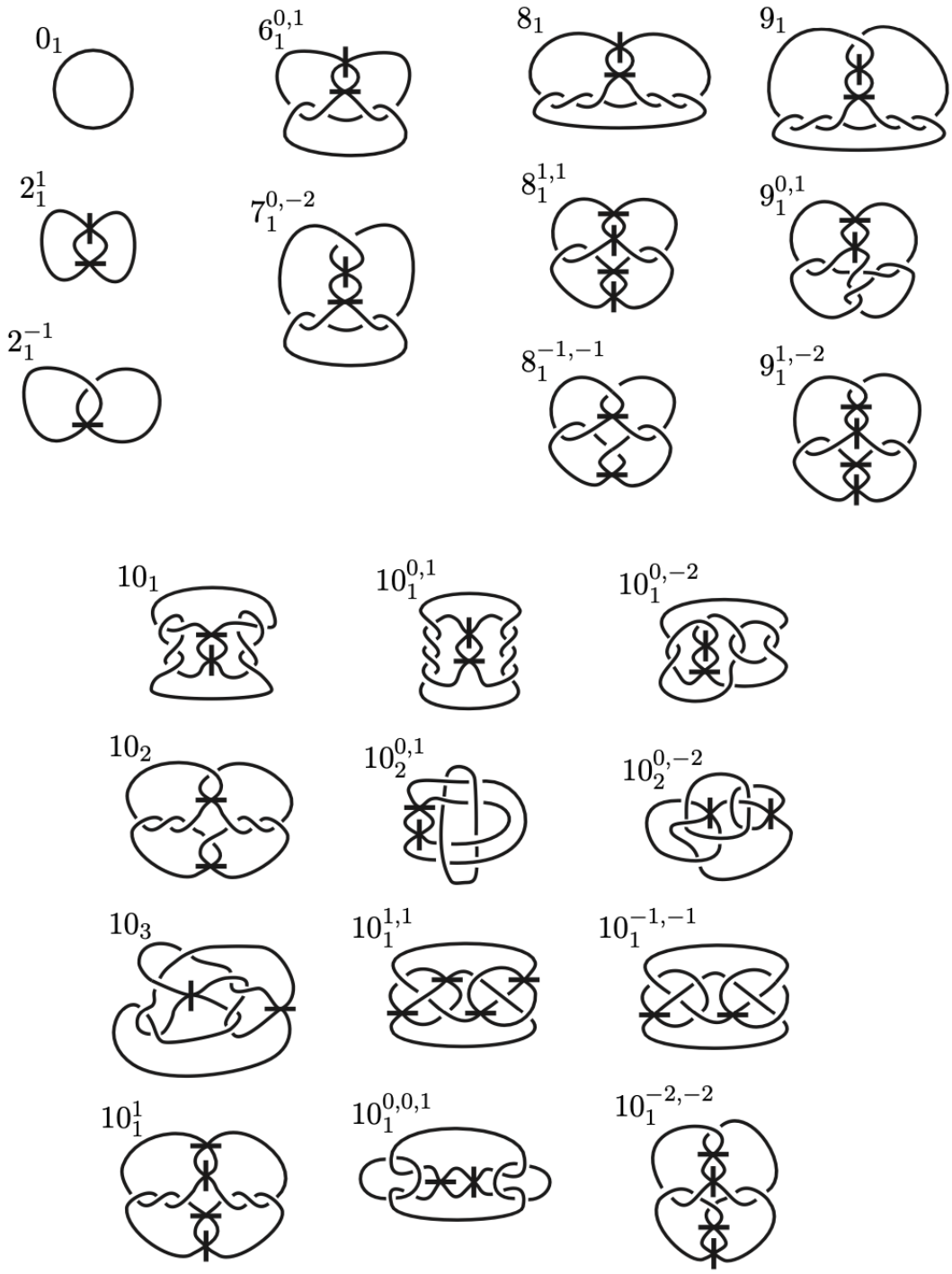

FIGURE 4.2. Author's rendition of Yoshikawa's table found in [63].

with the Reidemeister III moves in the motion picture. To generate a broken sheet diagram of the entire surface-link include sheets containing saddles for each saddle point in the motion picture.

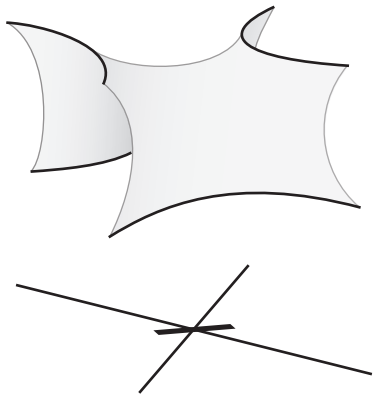

FIGURE 4.3. Induced saddle sheet.

Now, consider an admissible ch-diagram. There is a finite sequence of Reidemeister moves that takes L^- and L^+ to crossing-less diagrams O^- and O^+. Translate these Reidemeister moves to a broken sheet diagram. In between the still of L^- and L^+ and for each marked vertex include sheets containing the saddles traced by transitioning from L^- to L^+ in the local picture of Figure 4.1. These saddles are locally pictured in Figure 4.3. Finally, cap-off O^- and O^+ with trivial disks to produce a broken sheet diagram of a surface-link.

4.2. The Triple Point Numbers of Surface-Links Represented in Yoshikawa's Table

A surface-link F is *ribbon* if there is a trivial 2-link $\mathcal{O}$ and a collection of embedded (3-dimensional) 1-handles attaching to $\mathcal{O}$ such that F is the result of surgery along these 1-handles. These 1-handles intersect $\mathcal{O}$ only in their attaching regions. A surface-link with triple point number 0 is pseudo-ribbon.

The three trivial surface-knots 0_1, 2_1^1, and 2_1^{-1} are clearly pseudo-ribbon. Most of the remaining surface-links in Yoshikawa's table are ribbon.

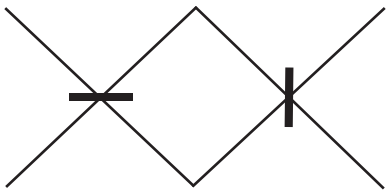

FIGURE 4.4. Marked vertex pattern.

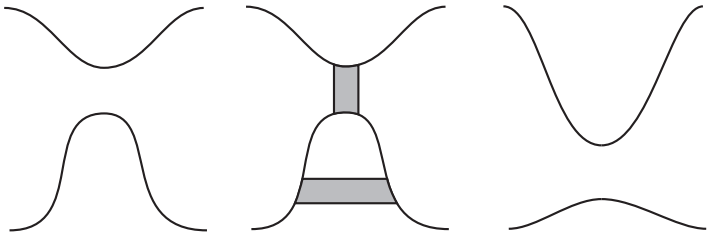

FIGURE 4.5. Motion picture of the saddles represented by Figure 4.4.

THEOREM 4.2.1. *Admissible ch-diagrams with vertices paired and isolated in the pattern of Figure 4.4 represent ribbon surface-links.*

PROOF. Figure 4.5 shows that the unlink diagrams of the positive and negative resolutions are identical, up to a small planar isotopy. The positive and negative resolutions are the boundary of trivial disk systems, families of disjoint 2-disks with one maximal (or minimal) point. Between these trivial disk systems include a product region representing the aforementioned small planar isotopies between the two resolutions to produce a collection of 2-knots each with just one minimal point and one maximal point. With no saddles, the constructed surface-link with all 2-sphere components is a trivial 2-link since any two trivial disk systems that have the same boundary are smoothly ambient isotopic (rel boundary) [38]. Figure 4.6 shows that the addition of the saddles represented by the marked vertices is equivalent to 1-handle surgery on this trivial 2-link.

□

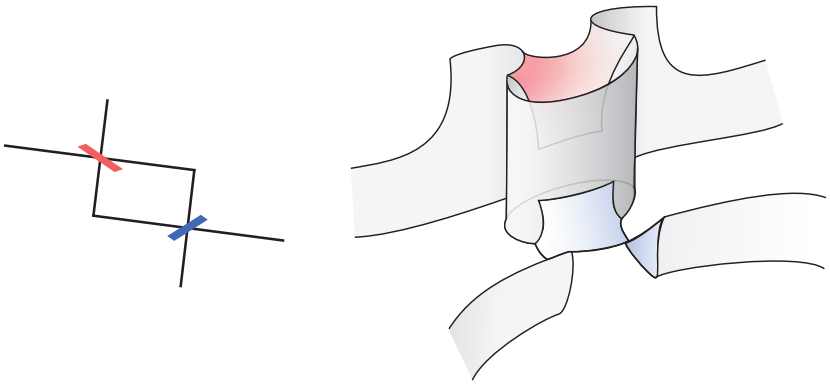

FIGURE 4.6. Ribbon handle associated with the given marked vertex pattern.

As a corollary to Theorem 4.2.1, all nontrivial surface-links of Yoshikawa's table except $8_1^{-1,-1}$, 10_2, 10_3, $10_1^{1,1}$, $10_2^{0,-2}$, and $10_1^{-1,-1}$ are ribbon.

THEOREM 4.2.2 (Satoh '01 [55], Kamada-Oshiro '09 [40]). *The triple point number of* $8_1^{-1,-1}$ *is 2.*

A surface in $\mathbb{R}^4$ is called $\mathbf{P}^2$-*irreducible* if it is not the connected sum $F_1 \# F_2$ where F_1 is any surface and F_2 is one of the two standard projective planes, i.e. 2_1^{-1} or its mirror. All surfaces in Yoshikawa's table except for 2_1^{-1} are irreducible, Section 5 of [63]. Satoh's lower bound calculation relies on each component being non-orientable, $\mathbf{P}^2$-irreducible, and having nonzero normal Euler number.

LEMMA 4.2.2.1 (Satoh '01 [55]). *For a* $\mathbf{P}^2$-*irreducible surface-link* $F = F_1 \cup \cdots \cup F_n$

$$t(F) \geq (|e(F_1)| + \cdots + |e(F_n)|)/2,$$

where $e(F_i)$ *denotes the normal Euler number of the surface-knot* F_i.

Kamada-Oshiro later proved $t(8_1^{-1,-1}) = 2$ using the symmetric quandle cocycle invariant. This method does not depend on the normal Euler number of the surface-link's components.

THEOREM 4.2.3 (Satoh-Shima '04 [59] '05 [60]). *The triple point number of the 2-twist-spun trefoil is 4, and the triple point number of the 3-twist-spun trefoil is 6.*

Since 10_2 represents the 2-twist-spun trefoil and 10_3 represents the 3-twist-spun trefoil, Satoh and Shima's results give $t(10_2) = 4$ and $t(10_3) = 6$.

THEOREM 4.2.4. *The surface-link* $10_1^{1,1}$ *is pseudo-ribbon.*

PROOF. Figure 4.7 shows that both the negative and positive resolutions of $10_1^{1,1}$'s marked vertex diagram only need Reidemeister II moves to achieve crossing-less diagrams. Thus, there is a broken sheet diagram representing $10_1^{1,1}$ with no triple points.

□

THEOREM 4.2.5. *The surface-link* $10_1^{-1,-1}$ *has a triple point number no greater than 12 and no less than 2.*

PROOF. Figures 4.10 and 4.11 illustrate a motion picture of $10_1^{-1,-1}$ whose induced broken sheet diagram has 12 triple points. Since $10_1^{-1,-1}$ is $\mathbf{P}^2$-irreducible [63] and each component is a projective plane, Lemma 5.4.2.1 implies that $2 \leq t(10_1^{-1,-1})$.

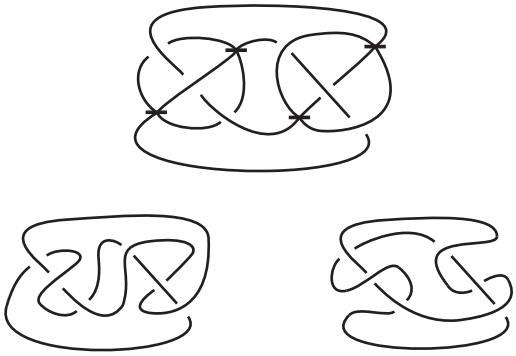

FIGURE 4.7. Negative and positive resolutions of $10_1^{1,1}$.

□

F	0_1	2_1^1	2_1^{-1}	$6_1^{0,1}$	$7_1^{0,-2}$	8_1	$8_1^{1,1}$	$8_1^{-1,-1}$	9_1	$9_1^{0,1}$
$t(F)$	0	0	0	0	0	0	0	2	0	0

F	$9_1^{1,-2}$	10_1	10_2	10_3	10_1^1	$10_1^{0,1}$	$10_2^{0,1}$	$10_1^{1,1}$	$10_1^{0,0,1}$
$t(F)$	0	0	4	6	0	0	0	0	0

F	$10_1^{0,-2}$	$10_2^{0,-2}$	$10_1^{-1,-1}$	$10_1^{-2,-2}$
$t(F)$	0	$t(10_2^{0,-2}) \leq 10$	$2 \leq t(10_1^{-1,-1}) \leq 12$	0

TABLE 4.1. Triple point number data on the surface-links represented in Yoshikawa's table [63].

THEOREM 4.2.6. *The surface-link* $10_2^{0,-2}$ *has a triple point number no greater than 10.*

PROOF. A motion picture of an induced broken sheet diagram of $10_2^{0,-2}$ is shown in Figure 4.9. This motion picture has 10 Reidemeister III moves that occur between the stills connected by an arrow.

□

REMARK 4.2.1. *Figure 4.9 shows that the Klein bottle component of* $10_2^{0,-2}$ *has a normal Euler number of 0. Therefore, Lemma 5.4.2.1 does not give a positive lower bound. The symmetric quandle cocycle invariant has proven useful for generating lower bounds on the triple point number*

*of non-orientable surface-links, see [**11**, **40**, **51**]. A symmetric quandle must have a good involution with a fixed point in order to color* $10_2^{0,-2}$. *The trivial symmetric quandles of [**52**] color* $10_2^{0,-2}$ *but the given symmetric quandle cocycles have a weight of 0 for all such coloring. The dihedral quandle* R_4 *colors* $10_2^{0,-2}$ *and the identity is a good involution of* R_4, *but there are no calculated symmetric quandle cocycles of* (R_4, id). *None of the other explicitly defined symmetric quandles of [**11**, **40**, **51**, **52**] color* $10_2^{0,-2}$ *or admit a coloring that gives a non-zero weight with the explicitly defined symmetric quandle cocycles.*

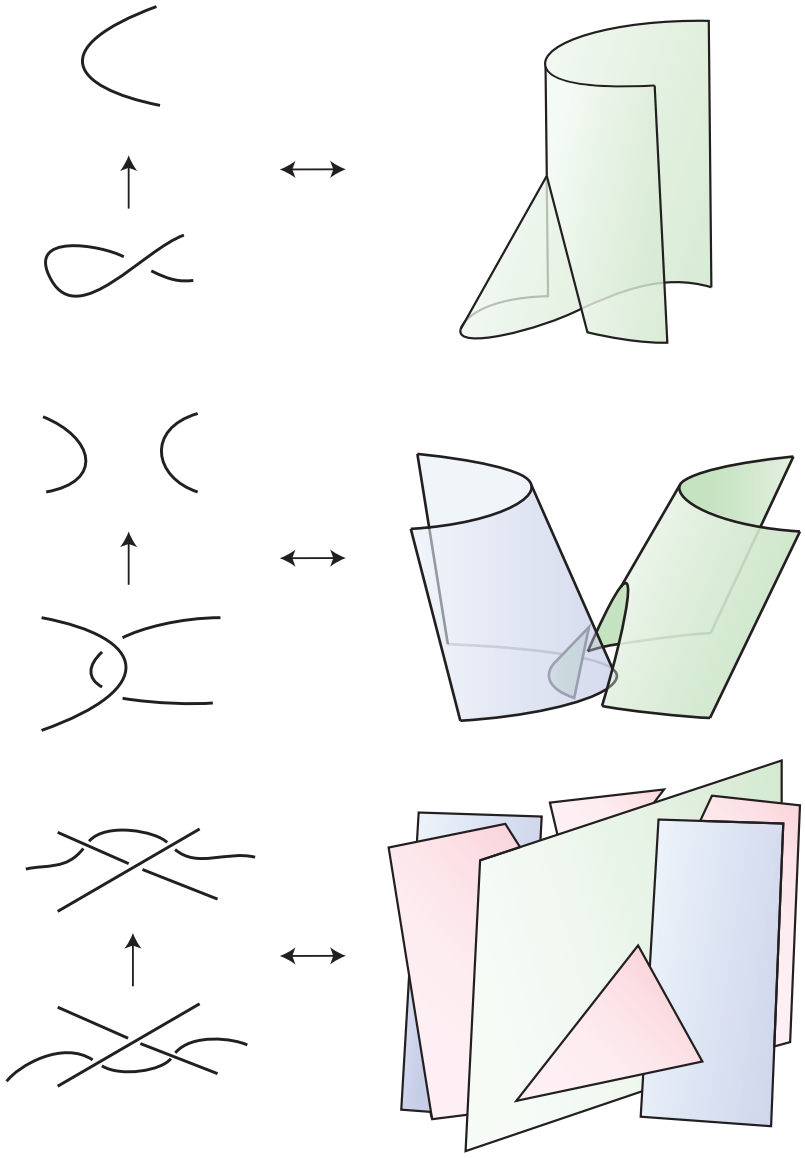

FIGURE 4.8. Relationship between Reidemeister moves in a motion picture and broken sheet diagrams.

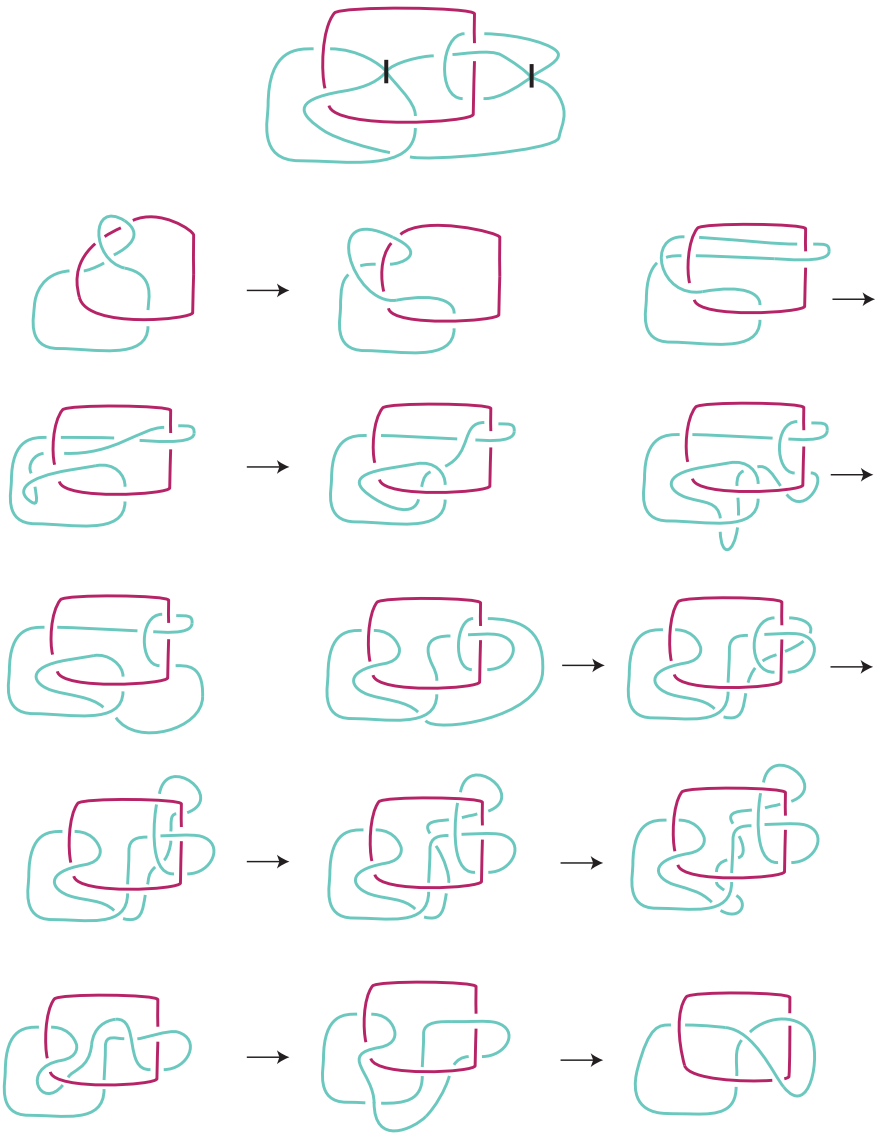

FIGURE 4.9. A motion picture of $10_2^{0,-2}$.

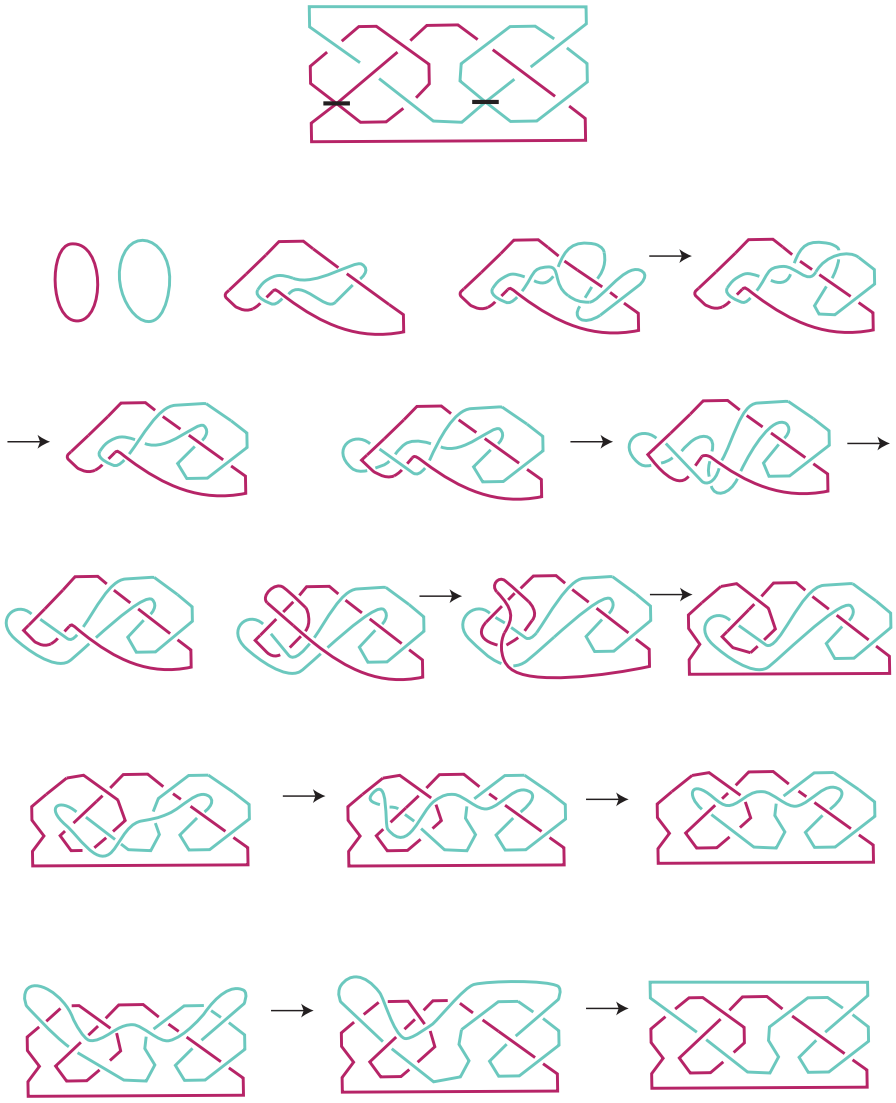

FIGURE 4.10. A motion picture of $10_1^{-1,-1}$, 1 of 2.

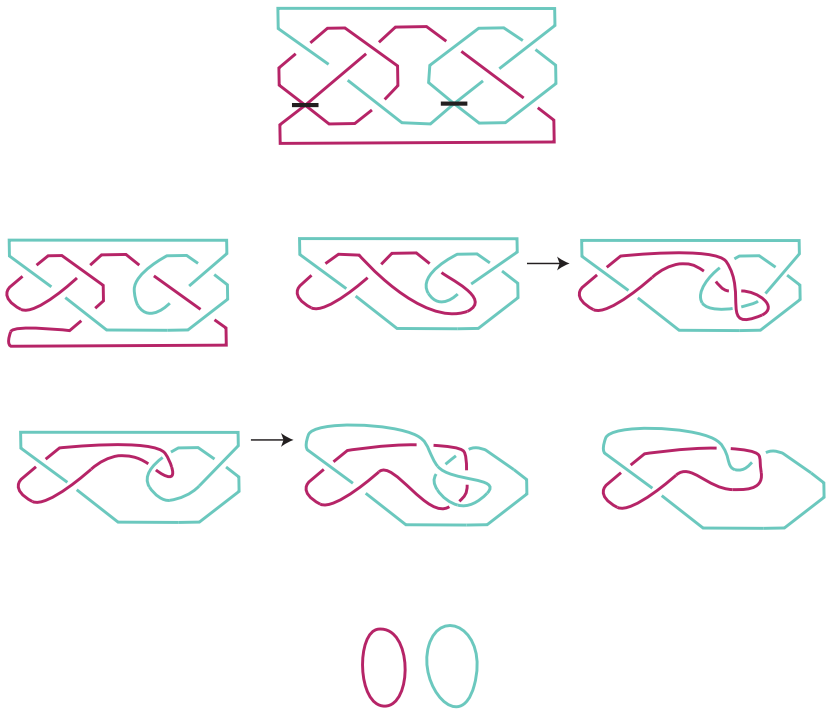

FIGURE 4.11. A motion picture of $10_1^{-1,-1}$, 2 of 2.

CHAPTER 5

The Shadow Quandle Cocycle Invariant of Knotoids

Shadow quandle coloring and the shadow quandle cocycle invariant were defined in [9]. In fact, a version of shadow quandle coloring of knotoid diagrams was defined, but the diagrams were called 1-knot arcs and the color of an endpoint arc equaled the color of its adjacent region. This was defined in the context of cross-sections of surface-links. This paper generalizes and reformulates the original definitions of shadow quandle coloring and the shadow quandle cocycle invariant of 1-knot arcs in the context of knotoids.

The shadow cocycle invariant is used to distinguishes the knot-type knotoid 3_1 from its mirror in Theorem 5.4.1. Moreover, the shadow coloring number and shadow cocycle invariant are used to distinguish infinitely many knotoids from their mirrors in Theorems 5.2.14 and 5.4.2.

Section 5.1 introduces knotoids and multi-linkoids, Section 5.2 defines the shadow coloring number of knotoids and uses it to distinguish infinitely many knotoids from their mirrors, Section 5.3 defines the shadow quandle cocycle invariant for knotoids, and Section 5.4 proves several chirality and crossing number results of knotoids and multi-linkoids using the invariant.

5.1. Knotoids

Knotoids are equivalence classes of knotoid diagrams.

DEFINITION 5.1.1. *A knotoid diagram κ in an orientable surface Σ is a generic immersion of the unit interval with crossing information given at each double point. Additionally, the image of 0 and 1 are distinct and called the head and leg of κ. A trivial knotoid diagram is an embedding of the unit interval.*

The three Reidemeister moves are defined on knotoid diagrams away from the head and leg. The supporting disk of the move is disjoint from either endpoint.

DEFINITION 5.1.2. *Consider the equivalence relation on knotoid diagrams generated by Reidemeister moves and planar isotopy. The equivalence classes of this relation are called knotoids. Knotoids in $\Sigma = S^2$ and $\Sigma = \mathbb{R}^2$ are referred to as classical.*

DEFINITION 5.1.3. *A classical knotoid is called a knot-type knotoid if it admits a diagram with both endpoints in the outer region.*

In S^2, a knotoid is a knot-type knotoid if it admits a diagram with both endpoints in the same region. Each knotoid has an associated knot by connecting the endpoints of any representative diagram by any generic simple arc that is given under crossing information wherever it meets the knotoid diagram. When a classical knotoid is knot-type then its invariants are closely related to the invariants of its associated knot.

DEFINITION 5.1.4 (Turaev '12 [62]). *Each knotoid diagram has a closed 2-disk neighborhood $B \subset \Sigma$ that meets the diagram along a radius of B. This neighborhood is called a regular neighborhood of the endpoints. Given knotoid diagrams D and D' representing the knotoids κ and κ', pick regular neighborhoods B and B' of the leg of κ and the head of κ'. Glue $\Sigma - Int(B)$ to $\Sigma^2 - Int(B')$ along a homeomorphism $\partial B \to \partial B'$ carrying the only point of $D \cap \partial B_1$ to the only point of $D' \cap \partial B_2$. This creates the product knotoid diagram DD' in $\Sigma \# \Sigma$. Moreover, this product is invariant of diagram, i.e. $\kappa\kappa' := DD'$ is a well-defined knotoid product for any diagrams D and D' of κ and κ'.*

Turaev also described that when the knotoids $\kappa \subset S^2$ and $\kappa' \subset S^2$ have diagrams D and D' such that the head of D' is adjacent to the outer region, a diagram of $\kappa\kappa'$ is given by concatenating D and D' at the leg of D and head of D' in a neighborhood of the leg of D. This concatenation gives a knotoid diagram DD' representing $\kappa\kappa'$.

DEFINITION 5.1.5. *A knotoid is prime if it cannot be written as a product of two non-trivial knotoids.*

Goundaroulis, Dorier, and Stasiak systematically classified prime classical knotoids up to five crossings [25]. This classification is up to orientation and the symmetry-related involutions mir$(\cdot)$, sym$(\cdot)$, and rot$(\cdot)$, see Figure 5.1. The *mirror reflection*, mir$(\cdot)$, changes each crossing. *Symmetry*, sym$(\cdot)$, reflects a knotoid diagram with respect to the vertical line $0 \times \mathbb{R} \subset \mathbb{R}^2$. The composition of mirror reflection and symmetry is called *rotation*, rot$(\cdot)$.

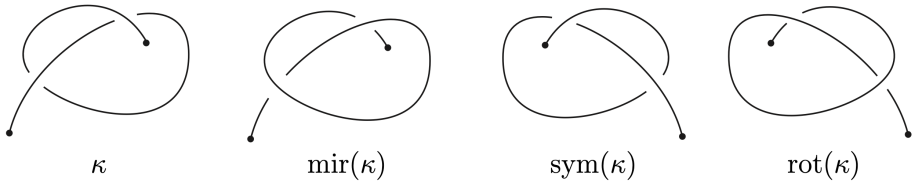

FIGURE 5.1. Involutions of a classical knotoid diagram.

They introduced a two-number notation of knotoids, analogous to the Rolfsen notation of knots and links. The first number represents the crossing number of the knotoid and the second number represents an index to distinguish knotoids in the same surface with the same crossing number. A knot-type knotoid is given the Rolfsen notation of its associated knot.

DEFINITION 5.1.6. *A multi-linkoid diagram in a closed surface Σ is a generic immersion of a number of unit intervals $[0,1]$ and circles S^1 into Σ. The images of the points 0 and 1 of the unit intervals are pairwise disjoint. Crossing information is given at every transverse double point.*

DEFINITION 5.1.7. *Consider the equivalence relation on multi-linkoids diagrams generated by Reidemeister moves away from the endpoints and planar isotopy. The equivalence classes of this relation are called multi-linkoids.*

5.2. Shadow Quandle Colorings of Knots and Knotoids

Recall:

DEFINITION 5.2.1. *A quandle is a set X with a binary operation $(x,y) \mapsto x^y$ such that*

(i) for any $x \in X$, it holds that $x^x = x$,

(ii) for any $x, y \in X$, there exists a unique $z \in X$ such that $z^y = x$, and

(iii) for any $x, y, z \in X$, it holds that $(x^y)^z = (x^z)^{(y^z)}$.

EXAMPLE 5.2.2. *The trivial quandle T_n of order n is determined by the relation $x^y = x$ for all $x, y \in E_n$.*

EXAMPLE 5.2.3. *For any group G, the relation $g^h = h^{-1}gh$ for all $g, h \in G$ defines a quandle on G called the conjugation quandle and $g^h = hg^{-1}h$ defines the core quandle.*

EXAMPLE 5.2.4. *Let Λ denote the ring of Laurent polynomials $\mathbb{Z}[t, t^{-1}]$. Let X be a left Λ-module, and define a quandle operation by $x^y = tx + (1-t)y$. This quandle is called the Alexander quandle.*

EXAMPLE 5.2.5. *The dihedral quandle $R_n = \mathbb{Z}/n\mathbb{Z}$ of order n is defined by $x^y = 2y - x$. The quandle operation can be calculated through the symmetries of regular n-gons. Let R_n be the vertices of the regular n-gon cyclicly ordered clockwise or counter-clockwise. For two points $x, y \in R_n$, the product x^y is the reflection of x across the line containing y and the center of the n-gon. See Figure 5.2.*

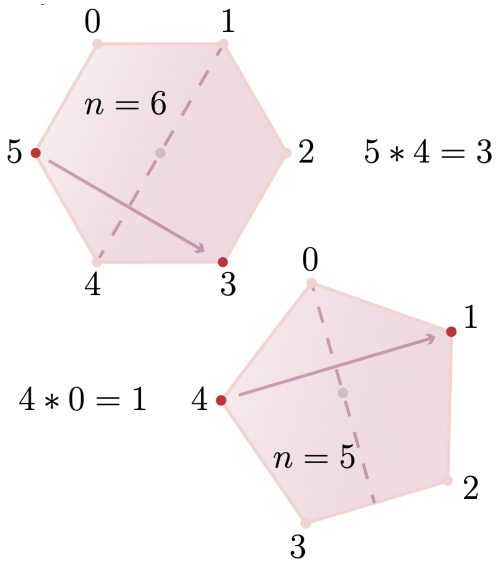

FIGURE 5.2. The dihedral quandle operation determined by the symmetries of a regular n-gon.

EXAMPLE 5.2.6. *There are only three quandles of order 3: T_3, R_3, and P_3. The multiplication table of P_3 is given in Table 5.1.*

P_3	0	1	2
0	0	0	0
1	2	1	1
2	1	2	2

TABLE 5.1. Multiplication table of P_3.

DEFINITION 5.2.7. *For a quandle X, a quandle coloring or X-coloring of an oriented knot or knotoid diagram is an assignment of X elements called colors to each arc such that the assignment satisfies the relation of Figure 5.3 at each crossing.*

The co-orientation normal is a more convenient orientation marking for verifying this relation. Given an oriented arc, the conventional normal vector direction is shown in Figure 5.3.

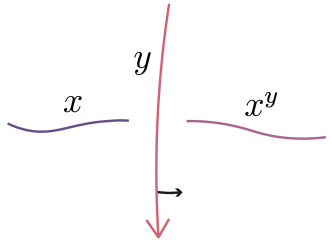

FIGURE 5.3. Quandle coloring condition around a crossing.

DEFINITION 5.2.8. *For a quandle X, an X-set is a set Y with a map $* : Y \times X \to Y; (y, x) \mapsto y*x$ satisfying the following conditions:*

(i) For any $x \in X$, $Y \to Y; y \mapsto y * x$ is a bijection.

(ii) For any $y \in Y$ and any $a, b \in X, (y * a) * b = (y * b) * (a * b)$.

Let D be the generic immersion of a knot into the plane. Since this projection is a 4-valent planar graph, the complement $\mathbb{R}^2 \setminus D$ (or $S^2 \setminus D$) is a collection of connected components called *regions*. The set of regions of D is denoted Region(D). With the addition of crossing information, the set of D's arcs is denoted Arc(D).

For a generic immersion of a knotoid into a surface $D \subset \Sigma$, $\Sigma \setminus D$ is a collection of connected components called *regions*, Region(D). With crossing information, D is a collection of arcs Arc(D); two arcs are distinct since they contain the head and leg.

DEFINITION 5.2.9. *Let X be a quandle and Y an X-set. For any oriented knot diagram D, an (X, Y)-coloring of D is a map $c : Arc(D) \cup Region(D) \to X \cup Y$ satisfying the following conditions:*

(i) $c(Arc(D)) \subset X$ and $c(Region(D)) \subset Y$.

(ii) The restriction of $c\big|_{Arc(D)} : Arc(D) \to X$ is an X-coloring of D.

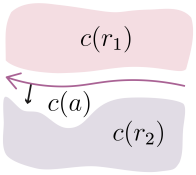

FIGURE 5.4. Coloring condition of region separated by an arc, $c(r_1)^{c(a)} = c(r_2)$.

(iii) Let r_1 and r_2 be adjacent regions of D along an arc $a \in Arc(D)$. If the co-orientation normal of a points from r_1 to r_2, then $c(r_1)^{c(a)} = c(r_2)$. See Figure 5.4.

Additional conditions are needed for knotoids:

DEFINITION 5.2.10. *Let X be a quandle and Y an X-set. For any oriented knotoid diagram D, an (X, Y)-coloring of D is a map $c : Arc(D) \cup Region(D) \to X \cup Y$ satisfying the following conditions:*

(i) $c(Arc(D)) \subset X$ and $c(Region(D)) \subset Y$.

(ii) The restriction of $c\big|_{Arc(D)} : Arc(D) \to X$ is an X-coloring of D.

(iii) Let r_1 and r_2 be adjacent regions of D along an arc $a \in Arc(D)$ that does not meet the head nor leg. If the co-orientation normal of a points from r_1 to r_2, then $c(r_1)^{c(a)} = c(r_2)$. See Figure 5.4.

(iv) Let r be the region of D adjacent to an arc $a \in Arc(D)$ that meets the head or leg. Regardless of orientation, $c(r)^{c(a)} = c(r)$. See Figure 5.5.

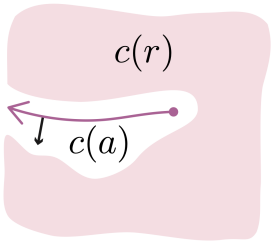

FIGURE 5.5. Coloring condition around an endpoint arc, $c(r)^{c(a)} = c(r)$.

An (X, Y)-coloring is also called a *shadow quandle coloring*.

DEFINITION 5.2.11. *The set of (X,Y)-colorings of a knot or knotoid diagram D is denoted $Col_{(X,Y)}(D)$. The size of $Col_{(X,Y)}(D)$, when finite, is denoted by $col_{(X,Y)}(D)$ and called the (X,Y)-coloring number or shadow coloring number by (X,Y).*

PROPOSITION 5.2.1 (Proposition 9.4.3 of [38]). *If two diagrams D and D' represent equivalent oriented knots, then there is a bijection between $Col_{(X,Y)}(D)$ and $Col_{(X,Y)}(D')$. The shadow coloring number $col_{(X,Y)}(D)$ is an invariant of an oriented knot.*

After a Reidemeister move on a (X,Y)-colored knot diagram there is a unique coloring extending the original. This establishes the bijection of the proposition.

PROPOSITION 5.2.2. *If two oriented knotoid diagrams D and D' represent equivalent knotoids, then there is a bijection between $Col_{(X,Y)}(D)$ and $Col_{(X,Y)}(D')$. The shadow coloring number $col_{(X,Y)}(D)$ is an invariant of a knotoid.*

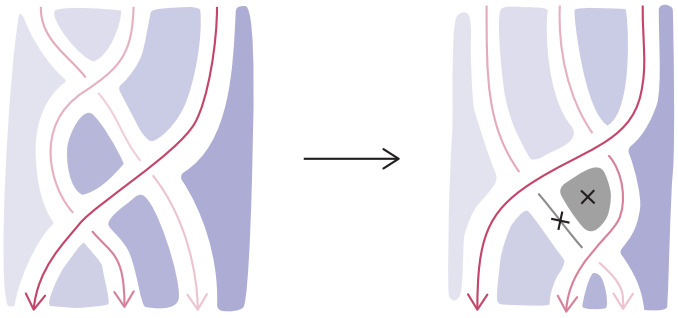

FIGURE 5.6. Marked arc and region created after a Reidemeister III move.

PROOF. This follows from the proof of the knot case, Proposition 5.2.1, seen in [9, 10, 38, 50]. After each Reidemeister move, there is a unique choice of color for any newly formed arc or region. For example, Figure 5.6 shows that after a Reidemeister III move there is a new region and arc created. Since a color z assigned to the new region or arc must satisfy the relation $z^x = y$ for known colors x and y, there exists a unique z by the condition (ii) of Definition 5.2.1. Similar arguments work in the simpler cases of Reidemeister I and II moves. Since Reidemeister moves on knotoid diagram occur away from the head and leg, these unique extension arguments apply for both knots and knotoids.

□

EXAMPLE 5.2.12. *For a quandle X, the number of X-colorings of a knotoid diagram D is an invariant denoted $col_X(D)$. The proof of this follows from the proof of the shadow coloring number's invariance. It's inferred from Figure 5.7 that $col_{R_n}(2_4) = col_{R_n}(3_2) = n$ while $col_{R_3}(mir(2_4)) > 3$ and $col_{R_5}(mir(3_2)) > 5$, i.e. 2_4 and 3_2 are chiral.*

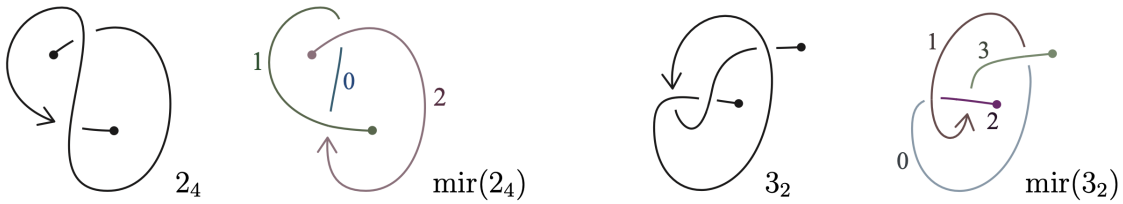

FIGURE 5.7. A 3-coloring of the planar knotoid $\text{mir}(2_4)$ and a 5-coloring of the classical knotoid $\text{mir}(3_2)$.

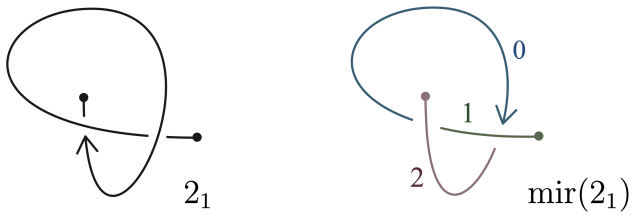

FIGURE 5.8. Knotoid diagrams of 2_1 and $\text{mir}(2_1)$.

EXAMPLE 5.2.13. *Consider the knotoid diagram of 2_1 in Figure 5.8. This diagram is (R_3, R_3)-colorable. Since $2y - x = x$ implies $y = x$ over $\mathbb{Z}/3\mathbb{Z}$, a choice of the infinite region's color determines the color of the head arc. The head arc and infinite region's color uniquely determines a shadow coloring, a trivial one. Therefore, $col_{(R_3,R_3)}(2_1) = 3$. Now consider the diagram of $mir(2_1)$ in Figure 5.8. This diagram is also (R_3, R_3)-colorable. As before, a choice of the infinite region's color determines the color of the head arc. A second choice of color for either remaining arc uniquely determines a (R_3, R_3)-coloring. Thus, $col_{(R_3,R_3)}(mir(2_1)) = 9$. Since $col_{(R_3,R_3)}(2_1) \neq col_{(R_3,R_3)}(mir(2_1))$, the classical knotoid 2_1 is chiral. Note, the standard 3-colorability makes this same distinction.*

THEOREM 5.2.14. *The shadow coloring number distinguishes infinitely many knotoids from their mirrors.*

PROOF. Consider the knotoid diagrams of the products $\prod_{i=1}^{n} 2_1$ and $\prod_{i=1}^{n} \text{mir}(2_1)$ in Figure 5.9. A recursion of 2_1 and $\text{mir}(2_1)$'s (R_3, R_3)-coloring choices determines the number of (R_3, R_3)-colorings of the products. In the case of $\prod_{i=1}^{n} 2_1$, the infinite region's color uniquely determines a trivial coloring as in Example 5.2.13. Therefore,

$$col_{(R_3,R_3)}\left(\prod_{i=1}^{n} 2_1\right) = 3.$$

In the case of $\prod_{i=1}^{n} \text{mir}(2_1)$, the infinite region's color only determines the head arc's color. There are 3 choices of colors for the remaining arcs of the first $\text{mir}(2_1)$ factor. This choice also colors the first arc of the second factor. There are 3 choices of colors for the remaining arcs of the second $\text{mir}(2_1)$ factor. This inductively continues for each factor. Once the arcs are colored, the infinite region's color determines the color of the remaining regions. Thus,

$$col_{(R_3,R_3)}\left(\prod_{i=1}^{n} \text{mir}(2_1)\right) = 3^{n+1}.$$

□

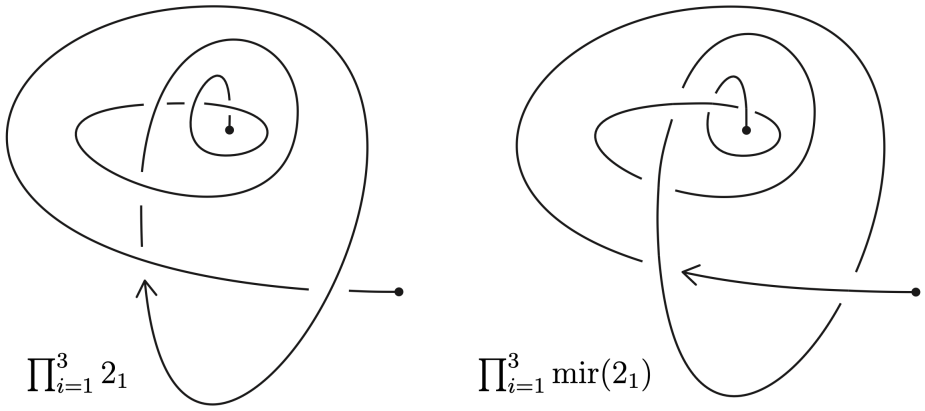

FIGURE 5.9. Product diagrams of 2_1 and $\text{mir}(2_1)$ powers.

REMARK 5.2.1. *Shadow quandle colorings and the shadow coloring number naturally extend to links and multi-linkoids.*

5.3. The Shadow Quandle Cocycle Invariant of Knots and Knotoids

Let X be a quandle and Y an X-set. Let $C_n^R(X)_Y$ denote the free abelian group generated by the elements of the Cartesian product $Y \times X^n$. When $n = 0$, $C_0^R(X)_Y = \mathbb{Z}[Y]$. If $n < 0$, then $C_n^R(X)_Y = 0$. Define a homomorphism $\partial_n : C_n^R(X)_Y \to C_{n-1}^R(X)_Y$ by

$$\partial_n(y, x_1, \ldots, x_n) = \sum_{i=1}^{n} (-1)^i (y, x_1, \ldots, \widehat{x}_i, \ldots, x_n) \\ - \sum_{i=1}^{n} (-1)^i (y * x_i, x_1^{x_i}, \ldots, x_{i-1}^{x_i}, \widehat{x}_i, x_{i+1}, \ldots, x_n).$$

Then $(C_n^R(X)_Y, \partial_n)$ is a chain complex [10, 22, 38, 50]. Let $C_n^D(X)_Y$ denote the subgroup of $C_n^R(X)_Y$ generated by all elements $(y, x_1, \ldots, x_n)$ such that $x_i = x_{i+1}$ for some i. For $n < 2$, put $C_n^D(X)_Y = 0$. Then $(C_n^D(X), \partial_n)$ is a chain sub-complex of $(C_n^R(X)_Y, \partial_n)$. Define $C_n^Q(X)_Y := C_n^R(X)_Y / C_n^D(X)_Y$ so that $(C_n^Q(X), \partial_n)_Y$ is a quotient complex. The homology groups of the chain complex $(C_n^Q(X), \partial_n)_Y$ are the *quandle homology groups* of X with an X-set Y.

Definition 5.3.1. *Let D be a diagram of an oriented knot or knotoid with co-orientation normals assigned to its arcs. Let v be a crossing of D. Among the four regions around v there is one such that both normals of its adjacent arcs point from the region. This region is called the specified region of v. A star will be placed in the corner of each crossing's specified region. The under arc adjacent to the specified region is called the specified arc.*

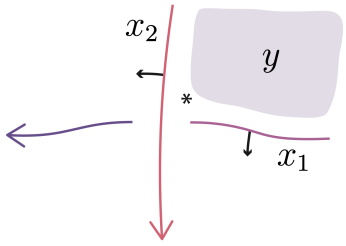

Figure 5.10. Starred specified region of a colored crossing.

Definition 5.3.2. *Let X be a quandle, Y an X-set, A an abelian group, $f \in Hom(C_2^R(X)_Y, A)$ a 2-cochain, and c an (X, Y)-coloring of an oriented knot or knotoid diagram D. For a crossing v*

of D, let $W_f(v,c) \in A$ be defined by

$$W_f(v,c) = \begin{cases} f(y,x_1,x_2) & \text{if } v \text{ is positive} \\ -f(y,x_1,x_2) & \text{if } v \text{ is negative,} \end{cases}$$

where (y,x_1,x_2) are the colors of the specified region, the specified under-arc, and the over-arc. The value $W_f(v,c)$ is called the local weight at v, and (y,x_1,x_2) is the color of the crossing. The f-weight of D is the total of the local weights and is denoted by

$$W_f(D,c) := \sum_v W_f(v,c).$$

DEFINITION 5.3.3. *If f satisfies the following two conditions, then the weight $W_f(D,c)$ is preserved under Reidemeister moves:*

(i) For any $y \in Y$ and any $x_1,x_2,x_3 \in X$,

$$\begin{aligned} &-f(y,x_2,x_3) + f(y*x_1,x_2,x_3) + f(y,x_1,x_3) \\ &-f(y*x_2,x_1^{x_2},x_3) - f(y,x_1,x_2) + f(y*x_3,x_1^{x_3},x_2^{x_3}) = 0 \end{aligned}$$

(ii) For any $y \in Y$ and $x \in X$, $f(y,x,x) = 0$.

In fact, these conditions are necessary and sufficient for a 2-cochain $f \in C_2^R(X)_Y \to A$ to be a 2-cocycle of the complex $Hom(C_*^Q(X)_Y, A)$ [10, 22, 38, 50]. Such a homomorphism $f : Y \times X^2 \to A$ satisfying the two conditions is called a quandle 2-cocycle of (X,Y).

THEOREM 5.3.4 (Theorem 9.4.5 of [38]). *Let f be a quandle 2-cocycle of (X,Y) and D an oriented diagram of a knot K. Define $\Phi_f(D) := \{W_f(D,c) | c \in Col_{(X,Y)}(D)\}$ as a multiset. It is an invariant of K, and if f and f' are cohomologous, then $\Phi_f(K) = \Phi_{f'}(K)$.*

For a subset $Y_0 \subset Y$, let $Col_{(X,Y)}(D)_{Y_0}$ denote the subset of $Col_{(X,Y)}(D)$ consisting of (X,Y)-colorings such that the infinite region is colored by elements of Y_0. Then

$$\Phi_f(D)_{Y_0} := \{W_f(D,c) | c \in Col_{(X,Y)}(D)_{Y_0}\}$$

is also an invariant.

THEOREM 5.3.5. *Let f be a quandle 2-cocycle of (X, Y) and D an oriented diagram of a knotoid κ. Define $\Phi_f(D) := \{W_f(D, c) | c \in Col_{(X,Y)}(D)_{Y_0}\}$ as a multiset. It is an invariant of κ, and if f and f' are cohomologous, then $\Phi_f(\kappa) = \Phi_{f'}(\kappa)$.*

PROOF. This follows from the proof of Theorem 5.3.4 seen in [9, 10, 22, 38, 50]. The proof of the former statement follows from analyzing the local weights of the crossings around a Reidemeister move. The f-weight does not change after a Reidemeister move. The proof of invariance among homology class representatives is a geometric consequence of examining the 1-cochain whose boundary is the difference $f - f'$.

□

DEFINITION 5.3.6. *Let D be a diagram of an oriented knot or knotoid. Let A be an abelian group written multiplicatively and X a finite quandle. For a quandle 2-cocycle f of (X, Y),*

$$\Phi'_f(D) := \sum_{c \in Col_{(X,Y)}(D)} \prod_v W_f(v, c)$$

is an element of the group ring $\mathbb{Z}[A]$ and is an invariant of an oriented knot. This invariant is called the shadow quandle cocycle invariant. For a subset $Y_0 \subset Y$, the invariant $\Phi'_f(D)_{Y_0}$ is also defined by restricting the colorings to $Col_{(X,Y)}(D)_{Y_0}$.

When $X = Y$, a *quandle 3-cocycle* of X is a quandle 2-cocycle of (X, Y).

DEFINITION 5.3.7. *Let X be a quandle, A an abelian group, and $\mathbb{Z}(X^3)$ the free $\mathbb{Z}$-module generated by the elements of $X^3 = X \times X \times X$. A homomorphism $f : \mathbb{Z}(X^3) \to A$ is a quandle 3-cocycle of X if the following conditions are satisfied:*

(i) For any $x_0, x_1, x_2, x_3 \in X$,

$$\begin{aligned} &- f(x_0, x_2, x_3) + f(x_0^{x_1}, x_2, x_3) + f(x_0, x_1, x_3) \\ &- f(x_0^{x_2}, x_1^{x_2}, x_3) - f(x_0, x_1, x_2) + f(x_0^{x_3}, x_1^{x_3}, x_2^{x_3}) = 0 \end{aligned}$$

(ii) For any $x, y \in X$, $f(y, x, x) = f(x, x, y) = 0$.

There is an associated chain and cochain complex of X. Quandle 3-cocycles are cocycles of this cochain complex and represent cohomology classes of $H^3_Q(X, A)$, see [7, 8, 10, 38, 50]. These

complexes are analogous to the complexes defined in the beginning of this section with the X-set Y omitted.

THEOREM 5.3.8 (Mochizuki '10 [47]). *Let $m > 0$ be any odd integer, and let p be any prime. Then, $H^3_Q(R_m, \mathbb{Z}_p) \cong \mathbb{Z}_p$ if m is divisible by p and $H^3_Q(R_m, \mathbb{Z}_p) \cong 0$ otherwise.*

EXAMPLE 5.3.9. *The cocycle $\theta_3 : R_3 \times R_3 \times R_3 \to \mathbb{Z}_3 = \langle u | u^3 = 1 \rangle$ given by*

$$\theta_3(x, y, z) = u^{(x-y)(y-z)z(x+z)}$$

generates $H^3_Q(R_3, \mathbb{Z}_3)$, and the cocycle $\theta_5 : R_5 \times R_5 \times R_5 \to \mathbb{Z}_5 = \langle t | t^5 = 1 \rangle$ given by

$$\theta_5(x, y, z) = t^{(y-x)(3z^5+2y^3z^2+2y^2z^3+3yz^4+3xy^4+3xy^3z+xy^2z^2+2xyz^3+4xz^4)}$$

generates $H^3_Q(R_5, \mathbb{Z}_5)$. These cocycles have been used to distinguish the trefoil from its mirror [53], to distinguish the 2-twist-spun trefoil from its mirror [7, 53], and to calculate the triple point numbers of the 2-twist-spun trefoil, 2-twist-spun figure-eight, and 2-twist-spun $(2, 5)$-torus knot [58, 59].

EXAMPLE 5.3.10. *Let $\phi : P_3 \times P_3 \times P_3 \to \mathbb{Z}_2 \oplus \mathbb{Z}$ be given by*

$$\phi(a, b, c) = \begin{cases} 1 \oplus 0 & (a, b, c) = (0, 1, 0), (0, 2, 0) \\ 0 \oplus 1 & (a, b, c) = (1, 0, 2), (2, 0, 1) \\ 0 \oplus -1 & (a, b, c) = (1, 0, 1), (2, 0, 2) \\ 0 \oplus 0 & \text{otherwise.} \end{cases}$$

The linear extension $\phi : \mathbb{Z}(P_3 \times P_3 \times P_3) \to \mathbb{Z}_2 \oplus \mathbb{Z}$ is quandle 3-cocycle of P_3. Oshiro used this linear extension as a symmetric quandle 3-cocycle to compute the triple point numbers of infinitely many non-orientable surface-links [51].

REMARK 5.3.1. *The shadow quandle cocycle invariant naturally extends to links and multi-linkoids.*

5.4. Applications of the Shadow Quandle Cocycle Invariant of Knotoids

THEOREM 5.4.1. *The knotoid 3_1 is chiral.*

PROOF. The knotoid diagrams of 3_1 and $\text{mir}(3_1)$ in Figure 5.11 are (R_3, R_3)-colored. Since $2y - x = x$ implies $y = x$ over $\mathbb{Z}/3\mathbb{Z}$, the infinite region's color determines the colors of the head and leg arcs. With $Y_0 = \{0\}$, the head and leg arcs must also be colored 0. Then, a choice of color for the marked arcs uniquely determines a (R_3, R_3)-coloring of the diagrams. Let c_i be the coloring determined by coloring the marked arc i. Therefore, $col_{(R_3,R_3)}(3_1)_{Y_0} = col_{(R_3,R_3)}(\text{mir}(3_1))_{Y_0} = 3$ with one trivial coloring and two non-trivial. The two non-trivial colorings differ by the permutation $0 \mapsto 0$, $1 \mapsto 2$, $2 \mapsto 1$ and are illustrated in Figure 5.11.

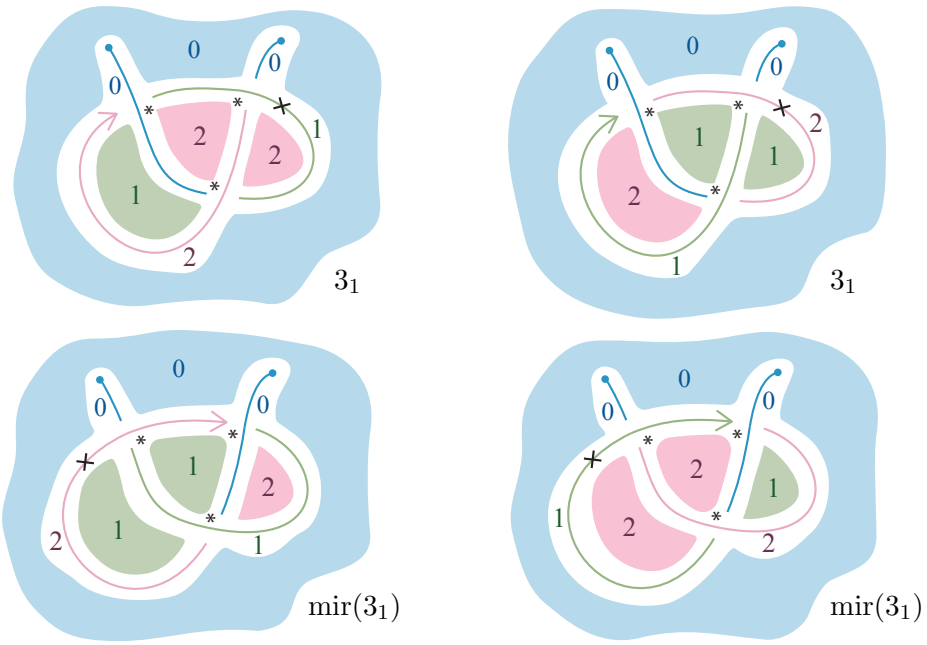

FIGURE 5.11. Non-trivial (R_3, R_3)-colorings of 3_1 and $\text{mir}(3_1)$ with $Y_0 = \{0\}$.

Recall that $\theta_3 : R_3 \times R_3 \times R_3 \to \mathbb{Z}_3 = \langle u | u^3 = 1 \rangle$ given by

$$\theta_3(x, y, z) = u^{(x-y)(y-z)z(x+z)}$$

generates $H^3_Q(R_3, \mathbb{Z}_3)$. For each coloring, Table 5.2 tabulates the 3-chains $\in C^Q_3(R_3)$ representing the sum of crossing colors and the θ_3-weights of each coloring.

With respect to (R_3, R_3), the shadow quandle cocycle invariants of these knotoids are

$$\Phi'_{\theta_3}(3_1)_{Y_0} = 1 + 2u^2 \in \mathbb{Z}[\mathbb{Z}_3],$$

c_i	Crossing Color Sum of 3_1	$W_{\theta_3}(3_1, c_i)$
c_0	$-(0,0,0)-(0,0,0)-(0,0,0)$	1
c_1	$-(2,2,1)-(2,0,2)-(2,1,0)$	u^2
c_2	$-(1,1,2)-(1,0,1)-(1,2,0)$	u^2

c_i	Crossing Color Sum of $\mathrm{mir}(3_1)$	$W_{\theta_3}(\mathrm{mir}(3_1), c_i)$
c_0	$(0,0,0)+(0,0,0)+(0,0,0)$	1
c_1	$(2,1,0)+(2,0,2)+(2,2,1)$	u
c_2	$(1,2,0)+(1,0,1)+(1,1,2)$	u

TABLE 5.2. (R_3, R_3)-colorings of 3_1 and $\mathrm{mir}(3_1)$.

and

$$\Phi'_{\theta_3}(\mathrm{mir}(3_1))_{Y_0} = 1 + 2u \in \mathbb{Z}[\mathbb{Z}_3].$$

□

COROLLARY 5.4.1. *For* $Y_0 = \{0\}$,

$$col_{(R_3,R_3)}\left(\prod_{i=1}^{n} \kappa_i\right)_{Y_0} = 3^n,$$

where each knotoid κ_i *is either* 3_1 *or mir*(3_1).

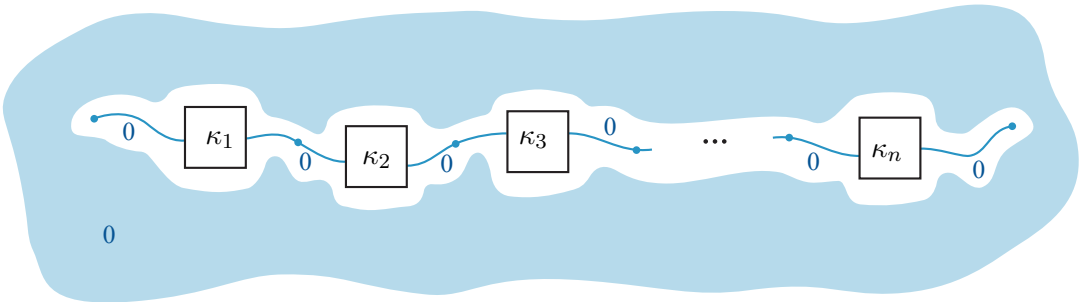

FIGURE 5.12. Knotoid product with 3_1 and $\mathrm{mir}(3_1)$ factors.

PROOF. Consider the knotoid diagram of $\prod_{i=1}^{n} \kappa_i$ in Figure 5.12. This diagram is seen as the concatenation of n diagrams from Figure 5.11 and is (R_3, R_3)-colorable. With $Y_0 = \{0\}$, there are

n independent choices of arc colors to uniquely determine a shadow coloring, the n marked arcs of each κ_i component seen in Figure 5.11.

□

THEOREM 5.4.2. *The shadow quandle cocycle invariant distinguishes infinitely many knot-type knotoids from their mirrors.*

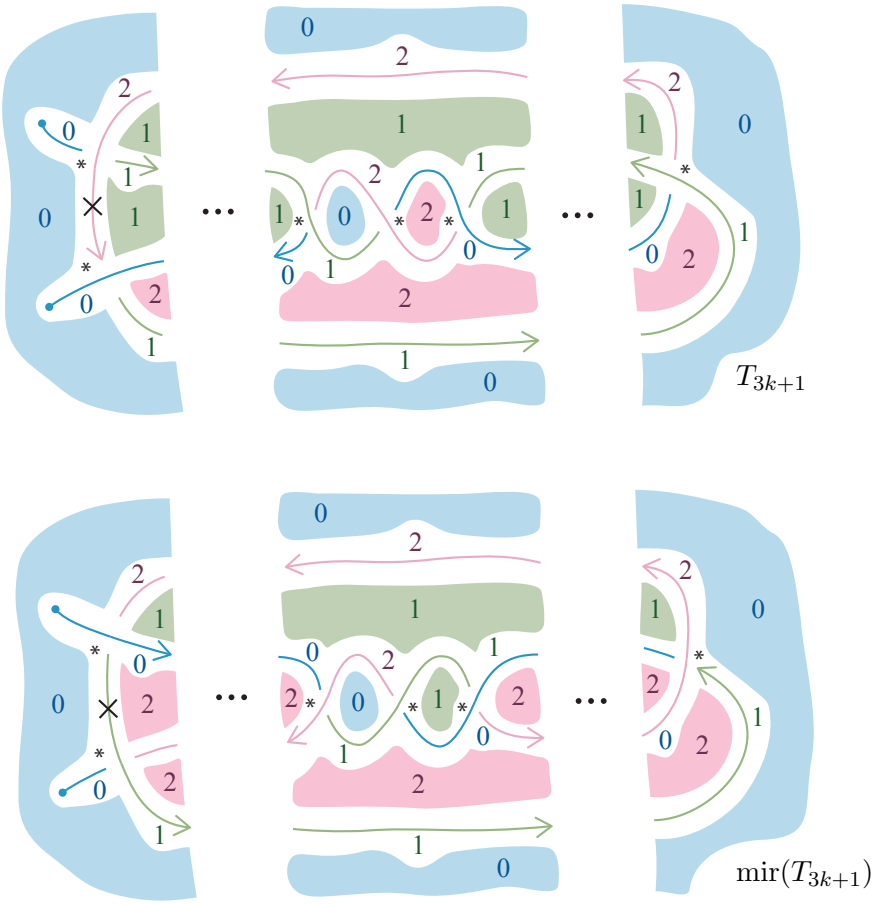

FIGURE 5.13. The colorings c_2 of T_{3k+1} and c_1 of mir(T_{3k+1}).

PROOF. For a non-negative integer k, consider the knotoid diagrams T_{3k+1} and mir(T_{3k+1}) shown in Figure 5.13. These diagrams represent knot-type knotoids and are (R_3, R_3)-colorable. Their associated knots are the $3k+1$-twist knot and its mirror. With $Y_0 = \{0\}$, the head and leg arcs must be colored 0 and a choice of color for the marked arc uniquely determines a (R_3, R_3)-coloring. Therefore, $col_{(R_3,R_3)}(T_{3k+1})_{Y_0} = col_{(R_3,R_3)}(\text{mir}(T_{3k+1}))_{Y_0} = 3$. The two non-trivial colorings differ

by the permutation $0 \mapsto 0$, $1 \mapsto 2$, $2 \mapsto 1$, one of which is shown in Figure 5.13. Let c_i denote the coloring determined by coloring the marked arc i in the diagrams of Figure 5.13.

These diagrams are drawn to show the repetition of the colorings every 3 twists. Each diagram will have k copies of the illustrated middle twisted region. Recall that $\theta_3 : R_3 \times R_3 \times R_3 \to \mathbb{Z}_3 = \langle u | u^3 = 1 \rangle$ given by

$$\theta_3(x, y, z) = u^{(x-y)(y-z)z(x+z)}$$

generates $H^3_Q(R_3, \mathbb{Z}_3)$. Suppose that $m \geq 0$ is a multiple of 9. Then, the crossing colors of the twisted region in T_{m+1} and $\mathrm{mir}(T_{m+1})$ come in multiples of 3 and do not contribute to the θ_3-weight of the diagram. Table 5.3 tabulates the crossing colors of the 3 crossings not in the m-twist region and the θ_3-weights of each coloring. This table shows that

$$\Phi'_{\theta_3}(T_{m+1})_{Y_0} = 1 + 2u^2 \in \mathbb{Z}[\mathbb{Z}_3],$$

and

$$\Phi'_{\theta_3}(\mathrm{mir}(T_{m+1}))_{Y_0} = 1 + 2u \in \mathbb{Z}[\mathbb{Z}_3].$$

c_i	Reduced Crossing Color Sum of T_{m+1}	$W_{\theta_3}(T_{m+1}, c_i)$
c_0	$(0,0,0) + (0,0,0) - (0,0,0)$	1
c_1	$(0,0,1) + (0,1,0) - (0,1,2)$	u^2
c_2	$(0,0,2) + (0,2,0) - (0,2,1)$	u^2

c_i	Reduced Crossing Color Sum of $\mathrm{mir}(T_{m+1})$	$W_{\theta_3}(\mathrm{mir}(T_{m+1}), c_i)$
c_0	$-(0,0,0) - (0,0,0) + (0,0,0)$	1
c_1	$-(0,1,0) - (0,0,1) + (0,1,2)$	u
c_2	$-(0,2,0) - (0,0,2) + (0,2,1)$	u

TABLE 5.3. (R_3, R_3)-colorings of T_{m+1} and $\mathrm{mir}(T_{m+1})$ with $Y_0 = \{0\}$.

□

For non-negative integers s and t, let $A_{s,t}$ denote the direct sum of s copies of $\mathbb{Z}_2$ and t copies of $\mathbb{Z}$, $A_{s,t} = (\mathbb{Z}_2)^s \oplus (\mathbb{Z})^t$. Every element of $A_{s,t}$ is of the form $(\alpha_1 \oplus \cdots \oplus \alpha_s) \oplus (\beta_1 \oplus \cdots \oplus \beta_t)$,

where α_i is an entry of the ith copy of $\mathbb{Z}_2$ and β_j is an entry of the jth copy of $\mathbb{Z}$. Let p_i and q_j be the elements of $A_{s,t}$ whose entries are all zeros except $\alpha_i = 1$ and $\beta_j = 1$.

LEMMA 5.4.2.1 (Kamda and Oshiro '09 [51]). *Let X be a quandle, and let $f : \mathbb{Z}(X^3) \to A_{s,t}$ be a 3-cocycle of X such that for any generator $(a, b, c) \in X^3$ of $\mathbb{Z}(X^3)$ it holds that*

$$f(a, b, c) \in \{0, p_i, \pm q_j\}.$$

If the f-weight $W_f(D, c)$ of a multi-linkoid diagram D with an (X, X)-coloring is equal to $(\alpha_1 \oplus \cdots \oplus \alpha_s) \oplus (\beta_1 \oplus \cdots \oplus \beta_t)$, then for the multi-linkoid μ representing D

$$c(\mu) \geq \sum_{i=1}^{s} \alpha_i + \sum_{i=1}^{t} |\beta_j|,$$

where the sum is taken in $\mathbb{Z}$ by regarding $\alpha_k = 0$ or 1 as an element of $\mathbb{Z}$.

The original statement and proof of Kamada and Oshiro's Lemma 5.4.2.1 is phrased in terms of triple points in broken sheet diagrams and the triple point number of surface-links [51]. Since a quandle 3-cocycle of X is a quandle 2-cocycle of (X, X) and the f-weight of knotoids is an invariant like the f-weight of surface-links, Lemma 5.4.2.1 is a valid reinterpretation of their result in the context of shadow quandle cocycles and knotoids.

Consider a multi-linkoid diagram realizing the crossing number of the multi-linkoid that it represents. If a 3-cocycle has $\mathbb{Z}$ coefficients and only takes the values $1, -1$ or 0, then the absolute value of the cocycle's weight cannot be greater than the number of crossings in the diagram. Since the weight of a quandle 3-cocycle is an invariant, the crossing number bounds the weight of the cocycle. This is the principle behind the lemma's proof.

THEOREM 5.4.3. *The shadow quandle cocycle invariant determines the crossing numbers of infinitely many multi-linkoids.*

PROOF. Take n trivial knotoids diagrams. Generically immerse one copy of S^1 that runs under each knotoid diagram once, creating positive crossings, then simply loops back. See Figure 5.14. Let M_n denote these multi-linkoid diagrams. These diagrams can be (P_3, P_3)-colored by coloring all arcs of the S^1 component 0, all knotoid diagrams 2, the region adjacent to the heads 2, and the region adjacent to the legs 1. Let c denote this shadow coloring and ϕ the 3-cocycle of P_3 defined

in Example 5.3.10. There are n positive crossings each colored $(1, 0, 2)$. Thus,

$$W_\phi(M_n, c) = 0 \oplus n \in \mathbb{Z}_2 \oplus \mathbb{Z}.$$

Lemma 5.4.2.1 implies that the crossing number of M_n is n. □

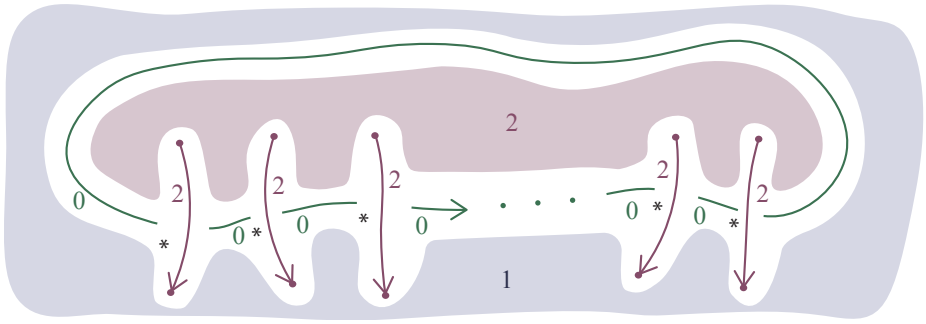

FIGURE 5.14. (P_3, P_3)-coloring of the multi-linkoids M_n.

Bibliography

[1] A. Al Kharusi and T. Yashiro, *No surface-knot of genus one has triple point number two*, Journal of Knot Theory and its Ramifications, 27 (2018), p. 1850063.

[2] A. Barbensi and D. Goundaroulis, *f-distance of knotoids and protein structure*, Proceedings of the Royal Society A, 477 (2021).

[3] V. Bardakov, P. Dey, and M. Singh, *Automorphism groups of quandles arising from groups*, Monatshefte für Mathematik, 184 (2017), pp. 519–530.

[4] V. Bardakov, T. Nasybullov, and M. Singh, *Automorphism groups of quandles and related groups*, Monatshefte für Mathematik, 189 (2019), pp. 1–21.

[5] J. Basi and C. Caprau, *Quandle coloring quivers of (p,2)-torus links*, Journal of Knot Theory and Its Ramifications, 31 (2022), p. 2250057.

[6] M. Bonatto, A. S. Crans, and G. Whitney, *On the structure of hom quandles*, Journal of Pure and Applied Algebra, 223 (2019), pp. 5017–5029.

[7] J. Carter, D. Jelsovsky, S. Kamada, L. Langford, and M. Saito, *Quandle cohomology and state-sum invariants of knotted curves and surfaces*, Transactions of the American Mathematical Society, 355 (2003), pp. 3947–3989.

[8] J. Carter, D. Jelsovsky, S. Kamada, and M. Saito, *Computations of quandle cocycle invariants of knotted curves and surfaces*, Advances in Mathematics, 157 (1999), pp. 36–94.

[9] J. Carter, S. Kamada, and M. Saito, *Geometric interpretations of quandle homology*, Journal of Knot Theory and Its Ramifications, 10 (2001), pp. 345–386.

[10] ——, *Surfaces in 4-Space*, Springer-Verlag Berlin Heidelberg, 2004.

[11] J. Carter, K. Oshiro, and M. Saito, *Symmetric extensions of dihedral quandles and triple points of non-orientable surfaces*, Topology and its Applications, 157 (2010), pp. 857–869.

[12] J. Carter and M. Saito, *Knotted surfaces and their diagrams*, American Mathematical Soc., 1997.

[13] ——, *Surfaces in 3-space that do not lift to embeddings in 4-space*, Banach Center Publications, 42 (1998), pp. 29–47.

[14] J. Carter, M. Saito, and S. Satoh, *Ribbon concordance of surface-knots via quandle cocycle invariants*, Journal of the Australian Mathematical Society, 80 (2006), pp. 131–147.

[15] N. Cazet, *Surface-link families with arbitrarily large triple point number*, Topology and its Applications, 319 (2022), p. 108234.

[16] ———, *On the triple point number of surface-links in yoshikawa's table*, Journal of Knot Theory and Its Ramifications, 32 (2023), p. 2350037.

[17] ———, *Quandles with one nontrivial column*, Journal of Algebra and Its Applications, (2023), p. 2550201.

[18] K. Cho and S. Nelson, *Quandle coloring quivers*, Journal of Knot Theory and Its Ramifications, 28 (2019), p. 1950001.

[19] A. Crans and S. Nelson, *Hom quandles*, Journal of Knot Theory and Its Ramifications, 23 (2014), p. 1450010.

[20] J. Dorier, D. Goundaroulis, F. Benedetti, and A. Stasiak, *Knoto-id: a tool to study the entanglement of open protein chains using the concept of knotoids*, Bioinformatics, 34 (2018), pp. 3402–3404.

[21] M. Elhamdadi, J. Macquarrie, and R. Restrepo, *Automorphism groups of quandles*, Journal of Algebra and its Applications, 11 (2012), p. 1250008.

[22] M. Elhamdadi and S. Nelson, *Quandles*, vol. 74, American Mathematical Soc., 2015.

[23] R. Fox, *A quick trip through knot theory*, Topology of 3-manifolds and related topics, (1962).

[24] D. Goundaroulis, J. Dorier, F. Benedetti, and A. Stasiak, *Studies of global and local entanglements of individual protein chains using the concept of knotoids*, Scientific reports, 7 (2017), pp. 1–9.

[25] D. Goundaroulis, J. Dorier, and A. Stasiak, *A systematic classification of knotoids on the plane and on the sphere*, arXiv preprint arXiv:1902.07277, (2019).

[26] D. Goundaroulis, N. Gügümcü, S. Lambropoulou, J. Dorier, A. Stasiak, and L. Kauffman, *Topological models for open-knotted protein chains using the concepts of knotoids and bonded knotoids*, Polymers, 9 (2017).

[27] N. Gügümcü and L. Kauffman, *New invariants of knotoids*, European Journal of Combinatorics, 65 (2017), pp. 186–229.

[28] N. Gügümcü and S. Lambropoulou, *Knotoids, braidoids and applications*, Symmetry, 9 (2017).

[29] N. Gügümcü and S. Nelson, *Biquandle coloring invariants of knotoids*, Journal of Knot Theory and its Ramifications, 28 (2019), p. 1950029.

[30] N. Gügümcü, S. Nelson, and N. Oyamaguchi, *Biquandle brackets and knotoids*, Journal of Knot Theory and Its Ramifications, 30 (2021), p. 2150064.

[31] E. Hatakenaka, *An estimate of the triple point numbers of surface-knots by quandle cocycle invariants*, Topology and its Applications, 139 (2004), pp. 129–144.

[32] X. Hou, *Automorphism groups of alexander quandles*, Journal of Algebra, 344 (2011), pp. 373–385.

[33] P. Jedlička, A. Pilitowska, D. Stanovskỳ, and A. Zamojska-Dzienio, *The structure of medial quandles*, Journal of Algebra, 443 (2015), pp. 300–334.

[34] P. Jedlička, A. Pilitowska, and A. Zamojska-Dzienio, *Subdirectly irreducible medial quandles*, Communications in Algebra, 46 (2018), pp. 4803–4829.

[35] D. Joyce, *A classifying invariant of knots, the knot quandle*, Journal of Pure and Applied Algebra, 23 (1982), pp. 37–65.

[36] S. Kamada, *2-dimensional braids and chart descriptions*, Topics in Knot Theory. NATO ASI Series, 399 (1993).

[37] ———, *Quandles with good involutions, their homologies and knot invariants*, Intelligence of low dimensional topology 2006, (2007), pp. 101–108.

[38] ———, *Surface-Knots in 4-Space*, Springer Monographs in Mathematics, Springer Singapore, 2017.

[39] S. Kamada, J. Kim, and S. Leem, *Computations of quandle cocycle invariants of surface-links using marked graph diagrams*, Journal of Knot Theory and Its Ramifications, 24 (2015).

[40] S. Kamada and K. Oshiro, *Homology groups of symmetric quandles and cocycle invariants of links and surface-links*, Transactions of the American Mathematical Society, 362 (2009).

[41] A. Kawauchi, T. Shibuya, and S. Suzuki, *Descriptions on surfaces in four space, i*, Mathematics Seminar Notes, 10 (1982).

[42] J. Kim, S. Nelson, and M. Seo, *Quandle coloring quivers of surface-links*, Journal of Knot Theory and Its Ramifications, 30 (2021), p. 2150002.

[43] D. Kodokostas and S. Lambropoulou, *Rail knotoids*, Journal of Knot Theory and Its Ramifications, 28 (2019).

[44] V. Lebed and A. Mortier, *Abelian quandles and quandles with abelian structure group*, Journal of Pure and Applied Algebra, 225 (2021), p. 106474.

[45] M. Manouras, S. Lambropoulou, and L. H. Kauffman, *Finite type invariants for knotoids*, European Journal of Combinatorics, 98 (2021), p. 103402.

[46] S. Matveev, *Distributive groupoids in knot theory*, Mat. Sb. (N.S.), 47 (1984), pp. 73–83.

[47] T. Mochizuki, *The third cohomology groups of dihedral quandles*, Journal of Knot Theory and Its Ramifications, 20 (2011), pp. 1041–1057.

[48] S. Nelson, *A polynomial invariant of finite quandles*, Journal of Algebra and Its Applications, 7 (2008), pp. 263–273.

[49] ———, *Generalized quandle polynomials*, Canadian Mathematical Bulletin, 54 (2011), pp. 147–158.

[50] T. Nosaka, *Quandles and Topological Pairs: Symmetry, Knots, and Cohomology*, Springer Singapore, 2017.

[51] K. Oshiro, *Triple point numbers of surface-links and symmetric quandle cocycle invariants*, Algebraic and Geometric Topology, 10 (2010), pp. 853 – 865.

[52] ———, *Homology groups of trivial quandles with good involutions and triple linking numbers of surface-links*, Journal of Knot Theory and Its Ramifications, 20 (2011), pp. 595–608.

[53] C. Rourke and B. Sanderson, *There are two 2-twist-spun trefoils*, Preprint, (2000).

[54] S. Satoh, *On non-orientable surfaces in 4-space which are projected with at most one triple point*, Proceedings of the American Mathematical Society, 128 (2000).

[55] ———, *Minimal triple point numbers of some non-orientable surface-links*, Pacific Jounral of Mathematics, 197 (2001).

[56] ———, *No 2-knot has triple point number two or three*, Osaka Journa of Mathematics, 42 (2005).

[57] ———, *Non-additivity for triple point numbers on the connected sum of surface-knots*, Proceedings of the American Mathematical Society, 133 (2005), pp. 613–616.

[58] ———, *The length of a 3–cocycle of the 5–dihedral quandle*, Algebraic and Geometric Topology, 16 (2016), pp. 3325–3359.

[59] S. Satoh and A. Shima, *The 2-twist-spun trefoil has the triple point number four*, Transactions of the American Mathematical Society, 356 (2004), pp. 1007–1024.

[60] ———, *Triple point numbers and quandle cocycle invariants of knotted surfaces in 4-space*, New Zealand Jounral of Mathematics, 34 (2005), pp. 71–79.

[61] Y. Taniguchi, *Quandle coloring quivers of links using dihedral quandles*, Journal of Knot Theory and Its Ramifications, 30 (2021), p. 2150011.

[62] V. Turaev, *Knotoids*, Osaka Journal of Mathematics, 49 (2012), pp. 195–223.

[63] K. Yoshikawa, *An enumeration of surfaces in four-space*, Osaka Journal of Mathematics, 31 (1994), pp. 497–522.

[64] B. Zhou and X. Liu, *Quandle coloring quivers of (p, 3)-torus links*, Journal of Knot Theory and Its Ramifications, (2023), p. 2350016.